Computed tomographic angiography in coronary artery disease

Patrick W. Serruys[1]*, MD, PhD; Nozomi Kotoku[1], MD; Bjarne L. Nørgaard[2], MD, PhD; Scot Garg[3], MD, PhD; Koen Nieman[4], MD, PhD; Marc R. Dweck[5], MD, PhD; Jeroen J. Bax[6,7], MD, PhD; Juhani Knuuti[6,7], MD, PhD; Jagat Narula[8], MD, PhD; Divaka Perera[9], MD, MB, BChir; Charles A. Taylor[10], PhD; Jonathon A. Leipsic[11], MD; Edward D. Nicol[12,13], MD; Nicolo Piazza[14], MD, PhD; Carl J. Schultz[15,16], MD, PhD; Kakuya Kitagawa[17], MD, PhD; Bernard De Bruyne[18,19], MD, PhD; Carlos Collet[18], MD, PhD; Kaoru Tanaka[20], MD, PhD; Saima Mushtaq[21], MD; Marta Belmonte[18], MD; Darius Dudek[22], MD, PhD; Adriana Zlahoda-Huzior[23,24], MSc; Shengxian Tu[25], PhD; William Wijns[1,26], MD, PhD; Faisal Sharif[1], MD, PhD; Matthew J. Budoff[27], MD; Johan de Mey[20], MD, PhD; Daniele Andreini[28,29], MD, PhD; Yoshinobu Onuma[1], MD, PhD

The authors' affiliations can be found in the Appendix paragraph.

P.W. Serruys and N. Kotoku contributed equally to this work.

This paper also includes supplementary data published online at: https://eurointervention.pcronline.com/doi/10.4244/EIJ-D-22-00776

Abstract

Coronary computed tomographic angiography (CCTA) is becoming the first-line investigation for establishing the presence of coronary artery disease and, with fractional flow reserve (FFR$_{CT}$), its haemodynamic significance. In patients without significant epicardial obstruction, its role is either to rule out atherosclerosis or to detect subclinical plaque that should be monitored for plaque progression/regression following prevention therapy and provide risk classification. Ischaemic non-obstructive coronary arteries are also expected to be assessed by non-invasive imaging, including CCTA. In patients with significant epicardial obstruction, CCTA can assist in planning revascularisation by determining the disease complexity, vessel size, lesion length and tissue composition of the atherosclerotic plaque, as well as the best fluoroscopic viewing angle; it may also help in selecting adjunctive percutaneous devices (e.g., rotational atherectomy) and in determining the best landing zone for stents or bypass grafts.

Corresponding author: Cardiovascular Research Centre for Advanced Imaging, Core Lab (CORRIB) Research Centre, University of Galway, University Road, Galway H91 TK33, Ireland. E-mail: patrick.w.j.c.serruys@gmail.com

Abbreviations

ACS	acute coronary syndrome
CABG	coronary artery bypass graft
CAC	coronary artery calcium
CAD	coronary artery disease
CCTA	coronary computed tomographic angiography
CTP	computed tomography perfusion
FFR	fractional flow reserve
FFR$_{CT}$	fractional flow reserve derived from coronary computed tomographic angiography
ICA	invasive coronary angiography
LAP	low-attenuation plaque
MACE	major adverse cardiac events
MI	myocardial infarction
MPI	myocardial perfusion imaging
NOCAD	non-obstructive coronary artery disease
PCI	percutaneous coronary intervention
PET	positron emission tomography
PTP	pretest probability
UHR-CT	ultra-high spatial resolution computed tomography

Introduction

During the nineties, coronary computed tomographic angiography (CCTA) emerged as a promising non-invasive imaging tool to diagnose coronary artery disease (CAD)[1], and two decades later, it has gained prominence as a first-line investigation in diagnosis and decision-making **(Central illustration, Supplementary Figure 1)**[1,2].

CAD phenotypes may be viewed as a pyramid of multiple layers of increasing anatomical complexity[3]. At the bottom are subjects with normal epicardial conductance vessels who have no atherosclerotic plaque and an excellent prognosis. Above them are patients with non-obstructive coronary plaque who have an increased risk of myocardial infarction (MI) and next, patients with progressive increases in plaque burden. Patients with normal coronary arteries or non-obstructive plaque may have structural or functional coronary microvascular dysfunction (CMD) that can lead to anginal symptoms with its two corollary syndromes (INOCA and ANOCA, i.e., ischaemia/angina with non-obstructive coronary arteries). Notably, "evidence of impaired coronary microvascular function should be present" with or without ischaemia[4].

PRETEST PROBABILITY FOR OBSTRUCTIVE CAD AND DIAGNOSTIC CCTA

The application of the pretest probability (PTP) for significant obstructive CAD (as determined by invasive coronary angiography [ICA] and fractional flow reserve [FFR]) based on age, sex, and the nature of symptoms underwent a major revision in the 2019 European Society of Cardiology (ESC) Guidelines for the diagnosis and management of chronic coronary syndromes (CCS)[5].

The PROMISE (Prospective Multicenter Imaging Study for Evaluation of Chest Pain) trial showed that in patients with a PTP <15%, the annual risk of cardiovascular death or MI was <1%[6].

The SCOT-HEART (Scottish Computed Tomography of the Heart) trial confirmed that the 2019 ESC estimates of PTP based on ICA and FFR were broadly similar to the prevalence observed on CCTA in the trial cohort[7], although it tended to underestimate the real prevalence, or alternatively, CCTA might overestimate the CAD **(Supplementary Figure 2A)**. The rates of 5-year cardiac death or non-fatal MI were 4.1%, 1.5% and 1.4% in patients with a PTP >15%, 5-15% and <5%, respectively (p<0.001 between groups) **(Supplementary Figure 2B)**.

On the other hand, the results of the Western Denmark Heart Registry, including 23,759 symptomatic patients, challenge the traditional dichotomous definition of CAD as "obstructive" or "non-obstructive" for identifying truly high-risk patients[8]. Major adverse cardiac events (MACE; MI, stroke, and all-cause death) at 4-year follow-up increased stepwise with both higher coronary artery calcium (CAC) scores and the number of vessels with obstructive disease detected by CCTA. Of note, when stratified into 5 groups according to CAC scores, the presence of obstructive CAD was not associated with a higher risk of MACE than the presence of non-obstructive CAD (NOCAD)[8].

Previously, the term "known CAD" had been used to define patients with a significant obstructive stenosis (i.e., ≥50%). In the recent American College of Cardiology (ACC)/American Heart Association (AHA) Chest Pain Guideline, the term "known CAD" was applied to those patients with prior anatomical testing (ICA or CCTA) with identified non-obstructive atherosclerotic plaque and obstructive CAD[9]. It was recognised as a "departure from convention" to ensure that those with lesser degrees of stenosis, who do not require revascularisation but who would benefit from optimised prevention therapy, do not get overlooked.
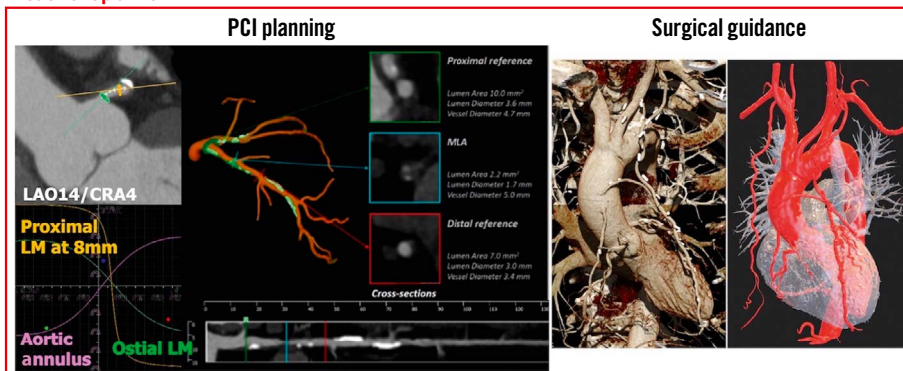
STRUCTURED REPORTING SYSTEM FOR CCTA

This year, the expert document 2022 Coronary Artery Disease-Reporting and Data System, or CAD-RADS 2.0, expanded on its first version, which was published in 2016 as a multi-society sponsored statement from the Society of Cardiovascular Computed Tomography (SCCT)/ACC/American College of Radiology (ACR)/ North American Society of Cardiovascular Imaging (NASCI) to standardise the reporting system for patients undergoing CCTA and to guide the possible next steps in patient management[10]. One key update provided in the CAD-RADS 2.0 statement is the estimation of coronary plaque burden; this is due to the emerging data supporting its stronger prognostic value over merely the presence or absence of an anatomical stenosis. In addition, there was a focus on physiological assessments of lesion-specific ischaemia using CT-derived FFR (FFR$_{CT}$) or CT perfusion (CTP).

The CAD-RADS score stratifies CAD stenosis severity as 0 (0%), 1 (1-24%), 2 (25-49%), 3 (50-69%), 4A (70-99% in 1 to 2 vessels), 4B (70-99% in 3 vessels or ≥50% in the left main), or 5 (100%). The additional description of P1 to P4 are used to indicate increasing categories of plaque burden. In the CONFIRM (Coronary CT Angiography Evaluation for Clinical Outcomes: An International Multicenter) registry, stratifying 5,039 patients

EuroIntervention

CENTRAL **ILLUSTRATION** The role of CCTA in coronary artery disease: a diagnostic tool, decision maker and treatment planner.
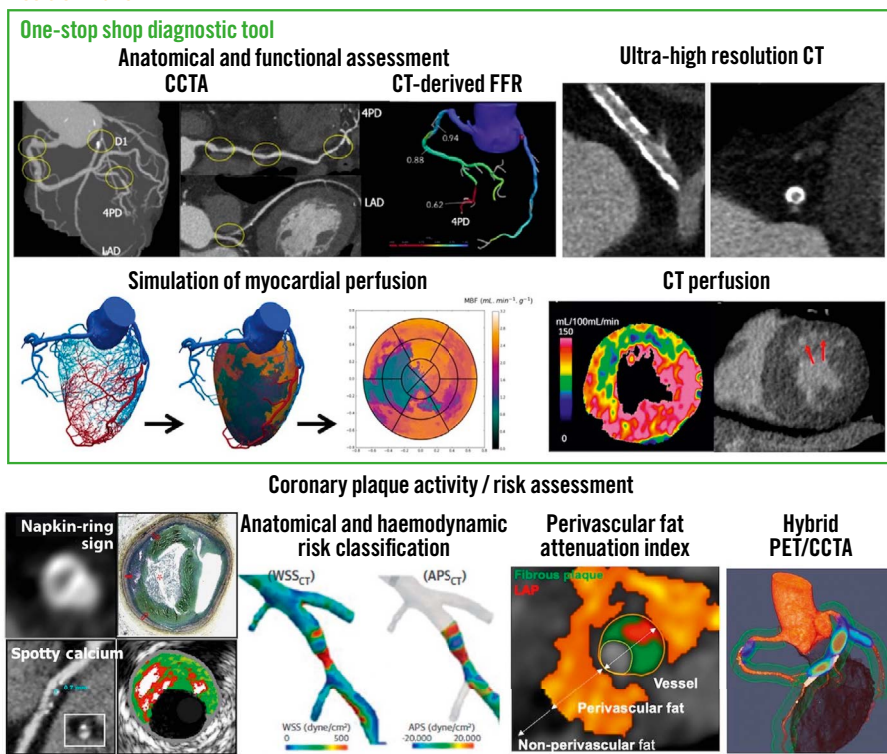
APS: axial plaque stress; CCTA: coronary computed tomographic angiography; CT: computed tomography; FFR: fractional flow reserve; LAD: left anterior descending; LM: left main; PCI: percutaneous coronary intervention; PET: positron emission tomography; WSS: wall shear stress

without known CAD by CAD-RADS scores, a multivariable Cox model demonstrated that CAD-RADS scores were strongly associated with an elevated risk for death or MI, with hazard ratios (HR) ranging from 2.46 for CAD-RADS 1 to 6.09 for CAD-RADS 5, using CAD-RADS 0 as the reference group (p<0.0001 for all comparisons)[11]. The prognostic implications of the CAD-RADS reporting system might be of no surprise since the CAD-RADS

score was designed to reflect CAD severity, therefore it is no wonder that it is associated with outcome.

The Coronary Artery Calcium Data and Reporting System (CAC-DRS) aimed at communicating the findings of CAC scanning on all non-contrast CT scans to facilitate clinical decision-making, with recommendations for subsequent patient management[12]. The CAC-DRS classified CAC based on Agatston scores as 0 (Agatston

score 0), 1 (1-99), 2 (100-299), and 3 (≥300), as well as on visual assessment. In the SCOT-HEART trial assessing 1,769 patients, patients classified as CAC-DRS 3 were at an increased risk of fatal or non-fatal MI compared to CAC-DRS 0 patients (HR 9.41, 95% confidence interval [CI] 3.24-27.31; p<0.001)[13].

Ultimately these structured reporting systems allow accurate communication of patient findings and convey prognosis, which may help provide guideline-based care directly from the CCTA findings.

RULING OUT CAD

Prospective multicentre studies investigating the diagnostic accuracy of CCTA for detecting a narrowing in an epicardial vessel in patients with suspected but unproven CAD have reported sensitivities of 85%-99% and specificities of 64%-92% **(Supplementary Table 1)**[1]. In a meta-analysis reported by Knuuti et al, when anatomical coronary narrowing >50% on ICA was considered a reference standard, CCTA had a sensitivity of 97%, a specificity of 78%, and substantial positive and negative likelihood ratios (4.44 and 0.04, respectively)[14] **(Supplementary Figure 3)**. Recent technological advancements have improved the diagnostic accuracy for detecting a significant coronary artery stenosis (≥50%), even in patients with atrial fibrillation and/or high heart rates, and photon-counting CT or ultra-high spatial resolution CT (UHR-CT) may further boost image resolution with inherent spectral information **(Supplementary Table 1)**[15,16].

UHR-CT provides a resolution of 150-200 µm and allows improved visualisation of calcified, stented, or small-diameter vessels[17] **(Figure 1)**. Using a commercially available UHR-CT, a recent study of high-risk patients with severe CAD as well as very high calcium scores (mean CAC score 1,205) provided promising preliminary data demonstrating a high diagnostic accuracy with a specificity of 88% in a per-vessel analysis compared with ICA **(Supplementary Table 1)**[15]. FFR$_{CT}$ is helpful in improving the dismal specificity of standard CCTA but does not improve the sensitivity of the technique. With the advent of UHR-CT, a significant reduction in false-positive findings may be expected and supersedes the need for an additional functional evaluation such as FFR$_{CT}$. Therefore, in this new era, the clinical role of FFR$_{CT}$ will have to be re-evaluated[18].

Furthermore, accurate evaluation of even smaller vessels with a diameter ≤400 µm may, in the future, help contribute to our understanding of CMD **(Supplementary Figure 4)**[18].

Despite its high diagnostic performance in large-scale trials, "the real-world performance of CCTA when interpreted by non-expert readers is less sanguine"[19]. In the PROMISE trial, including 4,347 patients, core laboratory and site interpretations were discordant in 16% of cases, with 80% (544 of 683) of these discordant interpretations in patients who had significant CAD (≥50% stenosis) by site but not by core laboratory interpretation[20]. Using data from the CREDENCE (Computed TomogRaphic Evaluation of Atherosclerotic DEtermiNants of Myocardial IsChEmia) trial, it was demonstrated that "Artificial intelligence (AI)-based evaluation of CCTA enables rapid and accurate identification and exclusion of high-grade stenosis, with a close agreement to blinded core lab-interpreted quantitative coronary angiography (QCA)" (intraclass correlation coefficient [ICC] 0.73 on a per-vessel basis; p<0.001)[19].

An international, multicentre study including 9 cohorts of patients undergoing CCTA at 11 sites showed excellent or good agreement between deep learning and expert reader measurements for total plaque volume (ICC 0.964) and percentage diameter stenosis (ICC 0.879; both p<0.0001)[21]. When compared with intravascular ultrasound (IVUS), there was also excellent agreement for deep learning total plaque volume (ICC 0.949) and minimal lumen area (ICC 0.904). A deep learning-based total plaque volume of ≥238.5 mm³ was associated with an increased risk of MI (HR 5.36, 95% CI: 1.70-16.86; p=0.0042). In this aspect,
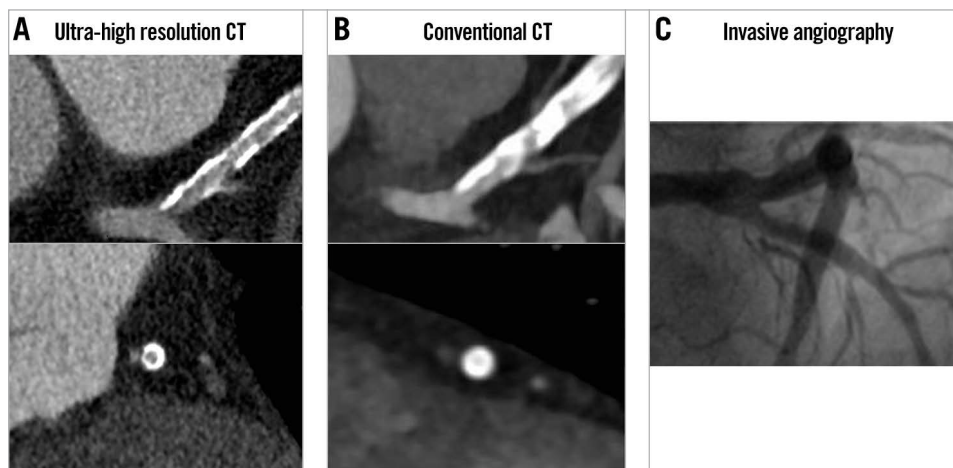
Figure 1. *Comparison between ultra-high resolution CT and conventional CT. A) In ultra-high resolution CT in a patient with a calcium score >2,000, the presence of a significant stenosis in the proximal LAD can be ruled out despite extensive calcifications. B) A significant lesion cannot be ruled out on conventional CT due to the substantial blooming artefacts. C) ICA confirmed the absence of significant stenosis. Reproduced with permission from[18]. CT: computed tomography; ICA: invasive coronary angiography; LAD: left anterior descending*

a standardised classification of CCTA results using CAD-RADS/CAC-DRS serves as the basis for developing AI.

However, a technique that currently provides an isotropic spatial resolution of approximately 0.25-0.50 mm has limitations in determining stenosis grade. In 4 mm vessels, the identifiable increments of percentage diameter stenosis are 6%. For smaller vessels, these increments are even larger. We may wonder whether this limited degree of precision in measuring percentage stenosis can be overcome by artificial intelligence despite the abovementioned evidence. Therefore, the CAD-RADS score used a degree of precision that may be at variance with the true physical reality.

In a prospective cohort study of 250 patients presenting to the emergency department, troponin-guided CCTA was evaluated in patients with suspected acute coronary syndrome (ACS) but a high-sensitivity cardiac troponin I concentration below the sex-specific 99th percentile – thus, after excluding non-ST-segment elevation MI (NSTEMI)[22]. This approach to using cardiac troponin to select patients for downstream CCTA after NSTEMI has been ruled out has the major potential to improve patient outcomes by accurately diagnosing CAD and guiding preventative treatments **(Figure 2)**.

Regarding the prognostic value derived from CCTA, in the SCOT-HEART trial, among the patients assigned to standard care plus CCTA, approximately half of the subsequent MI occurred among patients who had NOCAD[23]. In the PROMISE trial, the presence of high-risk plaque increased the rate of MACE (defined as death, MI, or unstable angina) among patients with NOCAD compared to patients without high-risk plaque[24]. The identification of high-risk non-obstructive plaque is a favourable addi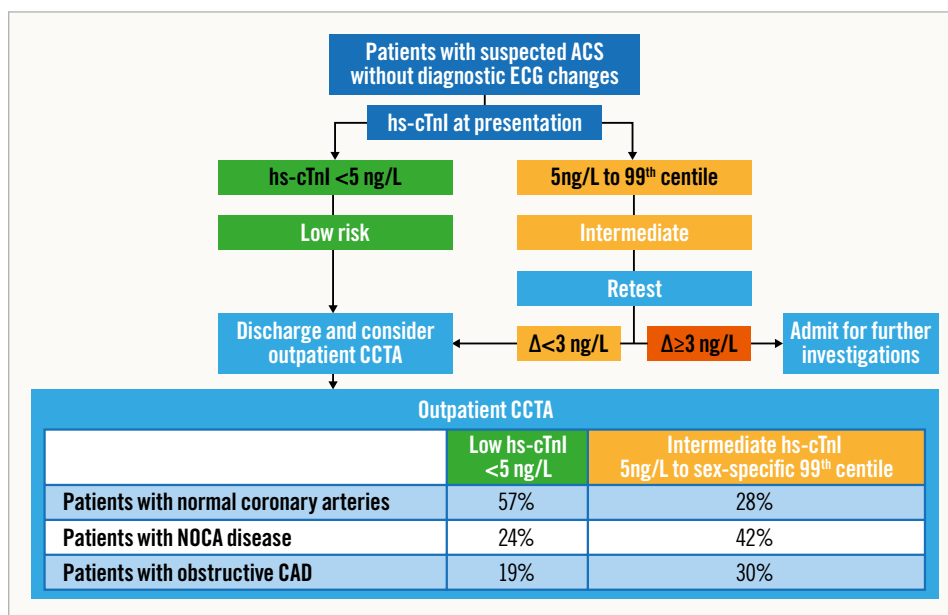tional benefit that comes with CCTA, which is missed by functional testing and not taken into account in the current PTP algorithm and may decisively lead to the use of preventative and aggressive pharmacological therapies[1].

In patients with ischaemic or non-ischaemic cardiomyopathy, cardiac CT also provides information on chamber size, function, and morphology and rules out obstructive CAD. Late enhancement CT imaging to evaluate myocardial viability in selected patients who cannot undergo cardiac magnetic resonance (CMR) could be useful if it impacts the diagnosis and decision-making. The details and limitations are described in the SCCT consensus document[25].

NON-INVASIVE FUNCTIONAL IMAGING: FFR$_{CT}$ AND MYOCARDIAL PERFUSION IMAGING

Diagnostic strategies to accurately rule out patients who do not require further testing are needed to offset the potentially higher ICA utilisation after CCTA as the first-line diagnostic workup[26]. Thus, guidelines recommend second-line function testing if CCTA suggests CAD of uncertain functional significance[5].

The prospective PACIFIC (Prospective Comparison of Cardiac PET/CT, SPECT/CT Perfusion Imaging and CT Coronary Angiography With Invasive Coronary Angiography) trial, including 208 patients with suspected CCS, showed that FFR$_{CT}$ "with adequate image quality of CCTA" had the largest area under the curve (AUC; 0.94) on a per-vessel comparison with CCTA alone (0.83), positron emission tomography (PET; 0.87), and single-photon emission computed tomography (SPECT; 0.70) when referenced to invasive FFR[27]. Adding SPECT or PET to CCTA alone improved the specificity, although, with a large loss in sensitivity (per-vessel: from 72% to 35% and 64%, respectively)[26].

	Low hs-cTnI <5 ng/L	Intermediate hs-cTnI 5ng/L to sex-specific 99th centile
Patients with normal coronary arteries	57%	28%
Patients with NOCA disease	24%	42%
Patients with obstructive CAD	19%	30%

Figure 2. *Troponin-guided CCTA. Reproduced with permission from[22]. ACS: acute coronary syndrome; CAD: coronary artery disease; CCTA: coronary computed tomographic angiography; ECG: electrocardiogram; hs-cTnI: high sensitivity cardiac troponin I concentrations; NOCA: non-obstructive coronary artery*

Findings from the Dan-NICAD 2 (Danish study of Non-Invasive testing in Coronary Artery Disease 2) trial[28] were presented at the 2022 ESC congress. Among 1,732 patients with symptoms suggestive of CAD, 26% of patients had ≥50% stenosis on CCTA and were referred for both 3-Tesla (3T) CMR or rubidium (Rb)-PET. Invasive FFR identified functional significance (≤0.80) in 41.1% of those patients with ≥50% stenosis on CCTA. The result showed discrepancy between the advanced myocardial perfusion imaging (MPI) and invasive FFR with sensitivities of 59% for 3T CMR and 64% for Rb-PET (p=0.21), while specificities were 84% and 89% (p=0.08), respectively, with invasive FFR ≤0.80 as the reference standard.

FFR_{CT} unlike MPI with SPECT/PET – is based on standard CCTA images from which patient-specific 3-dimensional (3D) anatomical and physiological models are derived, without the need for additional testing, medication, or radiation. Application of computational fluid dynamics principles enables computation of a 3D pressure map providing a physiological assessment of CAD at each point of the coronary tree[26], whereas MPI with SPECT/PET helps identify vessels with abnormal physiology but provides no pressure calculation, localisation of the pressure drop, nor characterisation of the physiological phenotype.

In the 2019 ESC Guidelines, CCTA with non-invasive functional imaging was given a class I level of evidence B recommendation as the initial test to diagnose CAD in symptomatic patients in whom obstructive CAD could not be excluded by clinical assessment alone[5]. In the recent ACC/AHA Chest Pain guidelines, CCTA received a class 2a recommendation for "determining atherosclerotic plaque burden and progression to obstructive CAD, and guiding therapeutic decision-making". FFR_{CT} was recommended (class 2a) down to the level of a 40% stenosis for the "diagnosis of vessel-specific ischaemia and to guide decision-making regarding the use of ICA"[9]. The forthcoming clinical use of CCTA as a "one-stop shop", including anatomical and physiological assessment to diagnose patients with new-onset chest pain **(Supplementary Figure 5)**, is also expected to serve as a decision-making tool.

The FORECAST (Fractional Flow Reserve Derived From Computed Tomography Coronary Angiography in the Assessment and Management of Stable Chest Pain) trial showed that a strategy of CCTA with selective FFR_{CT} in patients with stable angina was comparable with standard clinical care pathways in terms of cost and clinical outcomes at 9-month follow-up, and while reducing the use of ICA, it had no impact on decreasing coronary revascularisation[29,30]. The ADVANCE (Assessing Diagnostic Value of Non-invasive FFR_{CT} in Coronary Care) Registry reported 1-year clinical outcomes from real-world practice and provided safety data in patients with a negative FFR_{CT} for whom invasive evaluation was deferred. The results showed significantly lower rates of cardiovascular death or MI (0.20% vs 0.80%; relative risk [RR] 4.22, 95% CI: 1.28-13.95; p=0.01) with less revascularisation (5.60% vs 38.40%; RR 6.87, 95% CI: 5.59-8.45; p<0.001) in patients with an FFR_{CT} >0.80 compared to patients with an FFR_{CT} ≤0.80[31]. These abovementioned findings were further strengthened by a recent meta-analysis including five studies[32]. The 5-year follow-up of the NXT (Analysis of Coronary Blood Flow Using Coronary CT Angiography: Next steps) trial demonstrated that in patients with stable CAD, a positive FFR_{CT} (≤0.80) was a predictor of long-term MACE (cardiac death, non-fatal MI, or unplanned revascularisation) (HR 5.5; p=0.006) and was superior to an anatomically significant stenosis (≥50%) on CCTA[33].

Recently, there has been increasing interest in alternative, less demanding computational approaches that allow for on-site analysis. Comparisons of physiological models, computation time, and diagnostic performance between full-order and on-site CT-derived FFR are shown in **Figure 3** and **Supplementary Table 2**.

CT PERFUSION

FFR_{CT} benefits from the fact that analyses can be performed straight from the CCTA acquisition without additional scanning and pharmacological stressors; however, its diagnostic value in patients with previous MI, stents or bypasses remains to be established[26,34]. MPI including CTP remains a valuable alternative, although CTP is not used as a routine diagnostic tool in current clinical practice[25,35].

A meta-analysis of 54 articles and 5,330 patients indicated that CTP and its combined use with CCTA yielded a higher diagnostic performance (sensitivities 83% and 89%; specificities 79% and 81%, respectively) compared to CCTA alone, with an invasive FFR ≤0.80 as a standard reference[36].

The two primary methods of acquisition are static CTP and dynamic CTP with rest CCTA scanning followed by pharmacological stress or vice versa[37].

Static CTP acquires a single set of images during the first pass of contrast medium through the myocardium and during pharmacologically induced stress, providing a qualitative assessment – they are snapshots of myocardial iodine distribution and perfusion defects[25]. Perfusion defects are evaluated against baseline myocardial enhancement to determine reversibility and, hence, myocardial ischaemia, whereas an irreversible defect is indicative of infarcted tissue (e.g., scar tissue)[38].

Dynamic CTP requires a 2nd/3rd-generation dual-source or wide-detector CT system for complete myocardial coverage in one or two acquisitions with a higher radiation exposure than the static perfusion imaging[25]. By dynamic CTP, absolute myocardial blood flow (MBF) can be calculated from the time-attenuation curves (TAC), which are generated from a serial measurement of the attenuation values in the myocardium after injection of contrast medium **(Figure 4)**[38].

STATIC STRESS CTP

Although both technologies of CTP and FFR_{CT} are based on CT imaging, allowing anatomical and functional – perfusion or physiology – evaluation within 1 modality, CTP assesses the effects of both epicardial and microvascular perturbation, which is a different level of the ischaemic cascade from FFR_{CT}[34]. In the PERFECTION (PERfusion Versus Fractional Flow Reserve CT

Derived In Suspected CoroNary) study, the AUC to detect flow-limiting stenoses with CCTA, CCTA+FFR$_{CT}$, and CCTA+static stress-CTP were 0.89, 0.93, 0.92, respectively, in a vessel-based model, with significant additional values for CCTA+FFR$_{CT}$ and CCTA+static stress-CTP versus CCTA alone (p<0.001) but no difference between CCTA+FFR$_{CT}$ versus CCTA+static stress-CTP[39].
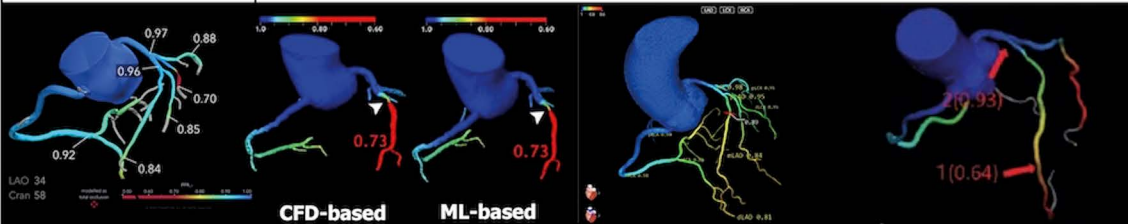
The Core320 (Combined Non-invasive Coronary Angiography and Myocardial Perfusion Imaging Using 320 Detector Computed Tomography) study compared the prognostic value of a combined anatomical/functional assessment by non-invasive imaging versus a traditional approach, showing that 5-year MACE (cardiac death, MI, hospitalisation for chest pain or congestive heart failure, and late revascularisation)-free survival rates were greater among patients with normal findings of combined CCTA-CTP compared to ICA-SPECT: 85% vs 80% (95% CI for difference: 0.1-11.3)[40].
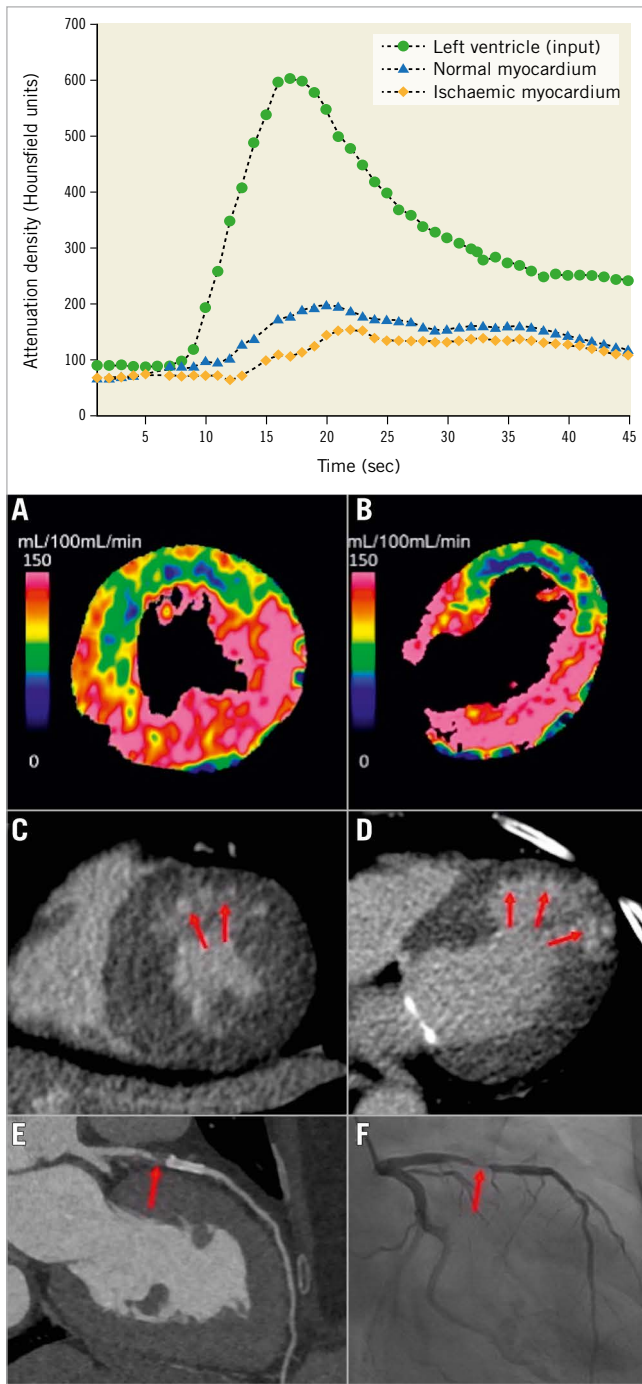
DYNAMIC CTP

The AMPLIFiED (Assessment of Myocardial Perfusion Linked to Infarction and Fibrosis Explored With Dual-Source CT) study showed that adding dynamic CTP to CCTA significantly increased the AUC from 0.65 (95% CI: 0.57-0.72) to 0.74 (95% CI: 0.66-0.81; p=0.011) at a patient level, with decreased sensitivity (93% vs 72%; p<0.001), improved specificity (36% vs 75%; p<0.001), and improved accuracy (64% vs 74%; p<0.001) when a haemodynamically significant stenosis was defined as an FFR of <0.8 or >90% stenosis during ICA[41] **(Figure 4)**. Of note, the addition of dynamic CTP to CCTA significantly increased the AUC from 0.80 to 0.84 (p=0.041) in 2-vessel disease (VD), and from 0.65 to 0.73 (p=0.022) in 3VD, but not in 1VD (from 0.84 to 0.87; p=0.265).

In the international SPECIFIC (Dynamic Stress Perfusion CT for Detection of Inducible Myocardial Ischemia) study investigating the diagnostic performance of dynamic stress CTP by 3rd-generation dual-source CT in addition to CCTA, diagnostic accuracy improved with the addition of CTP in vessels with a stenosis between 50-69% from 44% (95% CI: 33-55%) to 71% (95% CI: 61-81%) when stratified by stenosis grading on CCTA. This suggests that routine performance of CTP would not be justified in populations with low disease prevalence but may benefit after a CCTA which shows obstructive disease[42]. The CRESCENT 2 (Comprehensive Cardiac CT Versus Exercise Testing in Suspected Coronary Artery Disease 2) trial showed a higher diagnostic yield of subsequent ICA with an ESC class I indication for revascularisation (88% vs 50%; p=0.017) when CTP was selectively performed in patients with obstructive disease on CCTA, in comparison to

	HeartFlow FFR$_{CT}$	Siemens cFFR		Pulse CT-QFR	Canon CT-FFR
		Computational fluid dynamics-based	Machine learning-based		
3D anatomical model	≥**64** detector CT scanner				**320** detector CT scanner
Analysed vessel diameter in studies	>**1.8** mm	≥**1.5** mm		≥**1.5** mm	≥**1.8** mm
Physiological model Boundary conditions Microvascular resistance	Resting coronary flow (Q) by allometric scaling laws: $Q \propto$ myocardial mass Distribution of coronary flow over 3D model by Murray's law: $Q \propto d^3$ (d: vessel diameter) Patient-specific microvascular resistance (R): $R \propto d^{-3}$ Simulation of hyperaemic state by reducing the microvascular resistance			$Q \sim V^{\frac{3}{4}}$ (V: reference arterial volume) Conversion resting flow to virtual hyperaemic flow (HFV): $HFV = 0.10 + 1.55 \cdot RFV - 0.93 \cdot RFV^2$ (RFV: resting flow velocity)	Coronary flow: •Δ cross-sectional vessel area using 4 diastole phases Microvascular resistance: •minimised during diastole •constant resistance such that coronary pressure ∝ flow
Computation of flow Computational fluid dynamics (CFD) simulation of coronary flow	Full 3D CFD modelling by parallel supercomputer	Reduced-order CFD modelling by standard desktop computer			
Physiological model generation time	Full-order model within **4 hours** of data transfer	**30 to 60 min**		**17 min** (average)	39.4±8.6 min
Coronary flow computation time		**10 min**	**<2 sec**	**19 sec** (average)	

Figure 3. *Comparison between full-order and on-site CT-derived FFR. Functional diagnostic performance of full-order and on-site CT-derived FFR is shown in* **Supplementary Table 2**. *Modified and reproduced with permission from[90]. 3D: three-dimensional; cFFR: computed fractional flow reserve: CT: computed tomography; FFR: fractional flow reserve; FFR$_{CT}$: fractional flow reserve derived from coronary computed tomographic angiography; ML: machine learning; QFR: quantitative flow ratio*

Figure 4. *Dynamic myocardial perfusion imaging using dual-source CT and TAC. By dynamic CTP, absolute myocardial blood flow (MBF) can be calculated from the time-attenuation curves (TAC). Dynamic CTP showed reduced MBF in the LAD territory in both the (A) short-axis and (B) long-axis view (C,D) CT-delayed enhancement revealed a subendocardial infarction in the anterior wall within the reduced MBF area (red arrows). E) CCTA showed a high-grade stenosis in the LAD just proximal to the stent (red arrow). F) ICA revealed >90% stenosis (red arrow). Upper graph reproduced with permission from[38]. A-F) reproduced with permission from[41].*
CT: computed tomography; CCTA: coronary computed tomographic angiography; CTP: computed tomography perfusion; ICA: invasive coronary angiography; LAD: left anterior descending artery

standard functional testing (95% of functional testing was exercise electrocardiogram [ECG]), without increasing the rate of ICA[43].

Regardless of the CTP acquisition mode, the SCCT consensus document underlined the importance of patient selection and recommended adding CTP to CCTA when patients were at high atherosclerotic risk for obstructive CAD, including those with prior coronary intervention or significant calcification, or when there is a stenosis of indeterminate functional significance[37]. It also needs to be reassessed whether CTP with its associated radiation burden, in addition to CCTA, is still necessary when the use of UHR-CT, with a significant reduction in false-positive findings, will be more generalised in practice. Alternatives such as stress echocardiography or stress CMR perfusion imaging may be considered.

NOCAD AND MICROVASCULATURE DYSFUNCTION

Current explanations for INOCA reference either CMD or vasospastic angina, while in contrast, the recent US guidelines advocate ruling out the functional significance of diffuse atherosclerosis. Another independent explanation for INOCA is that it is related to the coronary lumen volume to myocardial mass ratio (V/M), measured non-invasively using CCTA. V/M provides an integrated measure of the balance between myocardial blood supply capacity and demand *in vivo*[44] **(Figure 5)**. In a *post hoc* analysis of the NXT trial including a total of 365 vessels in 202 patients with QCA stenosis ≤50%, multivariate logistic regression analysis, including percentage stenosis and quantitative plaque measures, demonstrated that V/M was an independent predictor of FFR ≤0.80[45], since V/M measures the same phenomenon in the whole coronary tree while FFR$_{CT}$ documents an epicardial phenomenon. An attempt to establish a relationship between V/M, FFR, and FFR$_{CT}$ has been made; however, this is not a measure of microvascular function. In fact, a substudy of the PACIFIC trial, investigating 431 vessels in 152 patients, found no association between V/M and vessel-specific hyperaemic MBF or coronary flow reserve (CFR) among vessels with NOCAD on ICA (361 vessels)[46].

Epicardial arteries, visualised by the "clinical angiographer", represent only 5% of the volume of the coronary tree, while pre-arterioles, arterioles, and capillaries represent 95% of the remaining coronary volume **(Supplementary Figure 4)**. The epicardial arteries (>400 µm) are the conduit vessels and might be interrogated by FFR, instantaneous wave-free ratio (iFR), and other non-hyperaemic pressure ratios[47]. The pre-arterioles (100-400 µm) and arterioles (40-100 µm) are involved in the regulation of flow distribution and in metabolic control, and the capillaries (<10 µm) are exchange vessels[48].

One approach to extend non-invasive physiological assessment from the epicardial coronary arteries to the microcirculation is to generate a synthetic tree following branching laws from the CCTA data down to the microvasculature. Recently, an algorithm for the generation of patient-specific cardiac vascular networks starting from segmented epicardial vessels down to the arterioles has been developed, with the potential to advance the non-invasive CCTA modelling of coronary flow, microvascular function, and
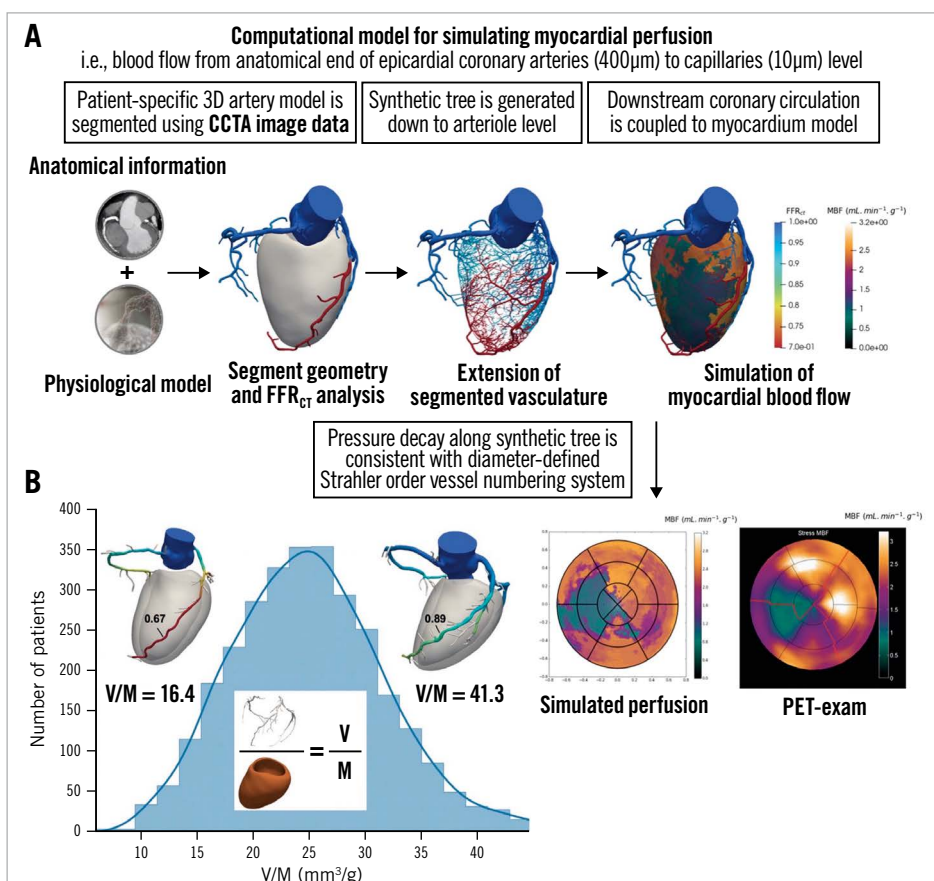
Figure 5. *Simulation of myocardial perfusion and coronary lumen volume to myocardial mass ratio. A) Approach to extend non-invasive physiological assessment from epicardial coronary arteries to microcirculation[50]. B) Coronary lumen volume to myocardial mass ratio (V/M). Reproduced with permission from[44]. CCTA: coronary computed tomographic angiography; FFR_CT: fractional flow reserve derived from coronary computed tomographic angiography; PET: positron emission tomography*

myocardial perfusion[44,49]. Papamanolis et al have described a computational model for simulating myocardial perfusion, i.e., blood flow from the anatomical end of the epicardial coronary arteries (400 μm) to the level of the capillaries (10 μm) **(Figure 5)**[50]. In this proof-of-concept paper, simulated MBF demonstrated favourable comparisons to $[^{15}O]H_2O$ PET data in five patients with NOCAD and in one patient with severe obstructive disease for both resting and hyperaemic conditions.

These innovative approaches will need to be evaluated in larger cohorts of patients to determine whether flow-modelling techniques based on CCTA anatomical data can provide insight into MBF as proven for non-invasive assessment of FFR. If this is successful, then CCTA might provide insight into both epicardial and microvascular disease.

SILENT CORONARY ATHEROSCLEROSIS DETECTED BY CCTA

The goal of the clinician is to match the intensity of preventive strategies with an individual's absolute risk of a future atherosclerotic cardiovascular disease event[51]. CCTA provides a comprehensive assessment of the entire coronary tree, including the presence of plaque, its morphology, and its extent[52].

SCAPIS (Swedish Cardiopulmonary Bioimage Study) recruited 30,154 randomly invited individuals aged 50 to 64 years who were not known to have CAD and had high-quality CCTA, showing that silent coronary atherosclerosis was common (42.1%), significant stenosis (≥50%) was less common (5.2%), and more severe forms, such as left main, proximal left anterior descending artery or 3VD, were rarely found (1.9%) in a middle-aged population[53]. In addition, CCTA-detected atherosclerosis increased with an increasing CAC score: all those with CAC >400 had atherosclerosis, of whom 45.7% had significant stenosis; 5.5% of those with 0 CAC had atherosclerosis, of whom 0.4% had significant stenosis, with increasing prevalence at higher baseline risk. The ACC/AHA guidelines on the primary prevention of cardiovascular disease recommend (IIa) measuring the CAC score to guide the clinician-patient risk discussion – not as a screening test – "in adults at intermediate risk, if risk-based decisions for preventive interventions remain uncertain", with the emphasis that the absence of CAC does not rule out non-calcified plaque, and that clinical judgment about risk should prevail[51]. Indeed, SCAPIS showed that in the population with 0 CAC, CCTA-detected atherosclerosis was present in 6.0% of patients with a strong family history of MI,

6.8% of those who were currently smokers, and 8.1% of those with diabetes[53].

In 2015 – prior to the 2022 CAD-RADS 2.0 statement, which focuses on the estimation of coronary plaque burden in addition to the severity of stenosis due to its strong association with incident coronary heart disease events[10] – the CT-adapted Leaman score (CT-LeSc), developed to quantify CCTA information about atherosclerotic burden (lesion localisation, degree of stenosis, and plaque composition), was validated as an independent long-term predictor of hard cardiac events[54] **(Figure 6)**. Patients with NOCAD and a CT-LeSc >5 had a similar risk of cardiovascular events when compared to patients with obstructive CAD (>50% stenosis) but a CT-LeSc <5[54]. In the CONFIRM registry, the 5-year prognostic value of the CT-LeSc was significant in patients without obstructive stenosis[55]. The Leiden group slightly modified the Leaman score by adding the subcategory "mixed plaque", in addition to calcified and non-calcified plaque[56] **(Figure 6)**. A higher Leiden CCTA risk score was associated with 5-year all-cause mortality or MI in the derivation (Leiden University Medical Center) and external validation cohort (the CONFIRM registry)[1,56].

It is noteworthy that most ACSs are caused by unstable but non-obstructive atherosclerotic plaque which cannot be identified by current invasive or non-invasive diagnostic tests detecting coronary luminal stenosis or stress-induced myocardial ischaemia[57]. The CRISP-CT (Cardiovascular RISk Prediction using Computed Tomography) study validated the prognostic role of the perivascular fat attenuation index (FAI), the first non-invasive biomarker of CCTA-detected "coronary inflammation", which is a driver of coronary atherosclerosis plaque formation and is a typical feature of plaque rupture, leading to ACS[57]. High perivascular FAI values (cut-off ≥−70.1 Hounsfield units [HU]) identify high-risk individuals with a 5- to 9-fold higher adjusted risk for cardiac death and, therefore, could guide early targeted primary prevention and intensive secondary prevention **(Supplementary Figure 6A)**.

HYBRID CCTA AND MOLECULAR PET

Moreover, analogous to the concept, ^{18}F-sodium fluoride (^{18}F-NaF) PET assesses atherosclerotic activity within the coronary arteries to complement the anatomical plaque imaging provided by CCTA **(Figure 7)**. Kwiecinski et al demonstrated that patients with a coronary microcalcification activity (CMA) >1.56 had a >7-fold increase in MI, independent of CAC and patient and lesion characteristics (HR 7.1, 95% CI: 2.2-25.1; p=0.003)[58]. The authors suggested that these patients might therefore be candidates for aggressive medical therapies, such as proprotein convertase substilisin kexin type-9 (PCSK9) or interleukin 1-beta inhibition. Other PET tracers are now being investigated for macrophage specificity and power to discriminate high-risk lesions, to provide information about active macrophages and coronary thrombus formation[59].

CCTA FOR CHARACTERISING PLAQUE AND MONITORING THE EFFECTS OF PLAQUE-MODIFYING TREATMENT

Novel semiautomated plaque quantification technology has facilitated quicker assessments and large-scale investigations, which have excellent correlation with IVUS[60]. Currently, three vendors have gained U.S. Food and Drug Administration clearance for AI-based coronary soft plaque assessment technologies (Cleerly; Elucid; and HeartFlow).
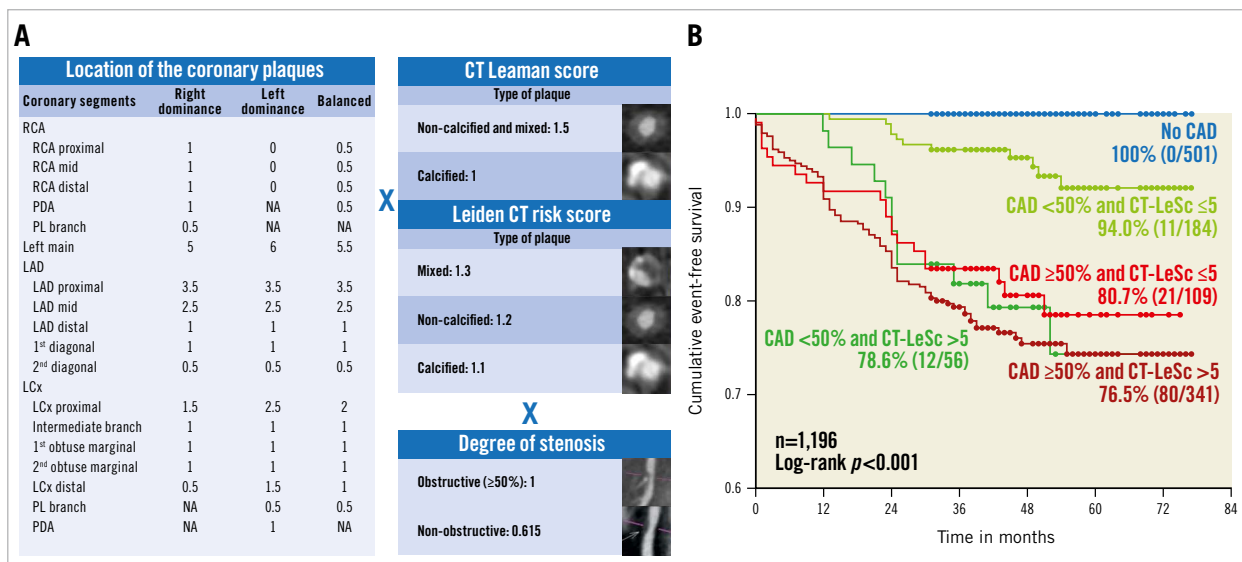
Figure 6. *CT Leaman score and Leiden CT risk score. A) Both are calculated by weighting for plaque localisation according to proximality or distality in the coronary circulation×type of plaque×stenosis severity. B) Kaplan-Meier survival curves for hard cardiac events stratified by obstructive versus non-obstructive CAD and CT Leaman score (CT-LeSc). Reproduced with permission from[54]. CAD: coronary artery disease; CT: computed tomography; LAD: left anterior descending artery; LCx: left circumflex; PDA: posterior descending artery; PL: posterolateral; RCA: right coronary artery*
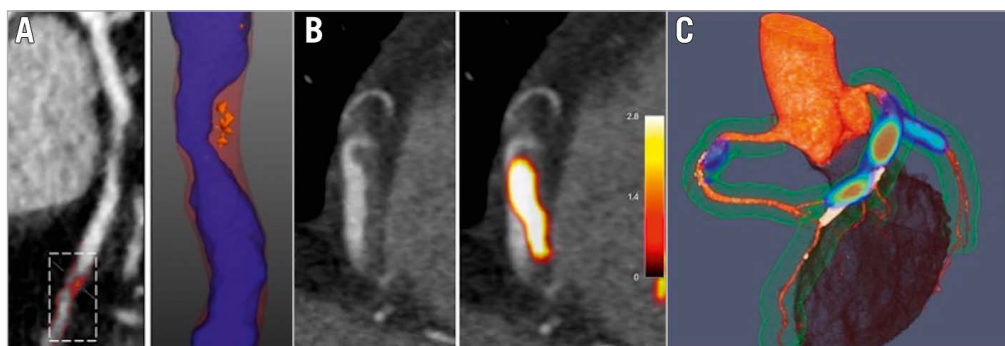
Figure 7. *Advanced assessments of plaque type, plaque thrombosis and disease activity with CT and hybrid PET/CT. A) CCTA with regions of LAP (<30 HU, orange areas) B) CCTA showing a low-density area in the lumen of RCA in a patient with inferior STEMI. Hybrid PET/CT images demonstrate 18F-GP1 activity as acute thrombus in this region (yellow area). C) Hybrid PET/CT image after administration of 18F-fluoride. Coloured areas represent regions of increased calcification activity. CT: computed tomography; CCTA: coronary computed tomographic angiography; HU: Hounsfield units; LAP: low-attenuation plaque; PET: positron emission tomography; RCA: right coronary artery; STEMI: ST-elevation myocardial infarction*

The PARADIGM (Progression of AtheRosclerotic PlAque Determined by Computed TomoGraphic Angiography Imaging) multinational prospective registry included 1,255 patients with suspected or known CAD undergoing CCTA at an interscan interval of ≥2 years[61]. The results showed that statin therapy was associated with a slower progression of coronary atherosclerosis volume, with increased calcification and a reduction of high-risk plaque features. In a multinational cohort study of 857 patients who underwent CCTA two or more years apart, van Rosendael et al performed quantitative measurements of coronary plaques throughout the entire coronary tree[62]. The results suggested an association of statin use with a greater rate of transformation of coronary atherosclerosis toward high-density calcium, supporting the concept of reduced atherosclerotic risk with increased density of calcium.

In a multicentre, observational study including 467 patients, Shin et al explored the relationship between the intensity of lipid-lowering treatments and changes in coronary plaque volume, demonstrating that patients with low-density lipoprotein cholesterol (LDL-C) <70 mg/dl had significantly slower plaque progression over 3 years compared with those with an LDL-C persisting ≥70 mg/dl at follow-up (12.7±38.2 mm^3 vs 44.2±73.6 mm^3; p=0.014)[63].

In addition to plaque volumetric changes as a surrogate marker of cardiovascular risk, the ROMICAT II (Rule Out Myocardial Ischemia/Infarction Using Computer Assisted Tomography II) trial showed the role of CCTA in the risk assessment of patients with high-risk plaque features[64]. While stenosis remained the strongest predictor of ACS in patients with acute chest pain, high-risk plaque (defined as positive remodelling [≥1.1], low-attenuation [<30 HU] area in plaque [LAP], napkin-ring sign, and spotty calcium) was associated with a 9-fold increase in the likelihood of ACS after adjusting for the presence of stenosis ≥50% and clinical risk assessment **(Figure 8A)**. In the SCOT-HEART trial, which followed up 1,769 patients for 5 years, LAP burden

was the strongest predictor of MI (adjusted HR 1.60, 95% CI: 1.10-2.34 per doubling; p=0.014), irrespective of cardiovascular risk score, CAC score, or coronary artery stenosis[65]. Patients with an LAP burden >4% concerning the total plaque burden were nearly 5 times more likely to have a subsequent MI (HR 4.65, 95% CI: 2.06-10.5; p<0.001). These results underscore the potential clinical interest of characterising the atherosclerotic burden, besides lumen stenosis, early in order to help identify patients with a higher risk of future cardiovascular events amenable to primary prevention[66].

The EVAPORATE (Effect of Vascepa on Improving Coronary Atherosclerosis in People With High Triglycerides Taking Statin Therapy) trial evaluated coronary plaque characteristics using CCTA to assess icosapent ethyl (IPE) as an adjunct to statin therapy and showed that IPE resulted in significant regression of LAP volume over 18 months (−0.3±1.5 mm^3 vs 0.9±1.7 mm^3; p=0.006)[67].

Patients with lipoprotein(a) [Lp(a)] concentrations, determined by the LPA gene for apolipoprotein(a) [apo(a)], higher than 150 nmol/l (approximately 60 mg/dl) comprise approximately 20% of the general population, and these patients are exposed to a greater risk of developing atherosclerotic cardiovascular disease and aortic stenosis[68]. The FOURIER (Further Cardiovascular Outcomes Research With PCSK9 Inhibition in Subjects With Elevated Risk) and ODYSSEY Outcomes (Evaluation of Cardiovascular Outcomes After an Acute Coronary Syndrome During Treatment With Alirocumab) trials showed that Lp(a) lowering by PCSK9 inhibitors was associated with a reduction in the rate of cardiovascular events in secondary prevention[69,70]. Kaiser et al showed that high concentrations of Lp(a) were associated with the progression of LAP on CCTA in patients with advanced multivessel CAD despite guideline-based preventative therapies[71]. This observation put forward a potential mechanism for the association between Lp(a) and the residual risk of MI, supporting Lp(a) as a novel target for treatment in atherosclerosis.
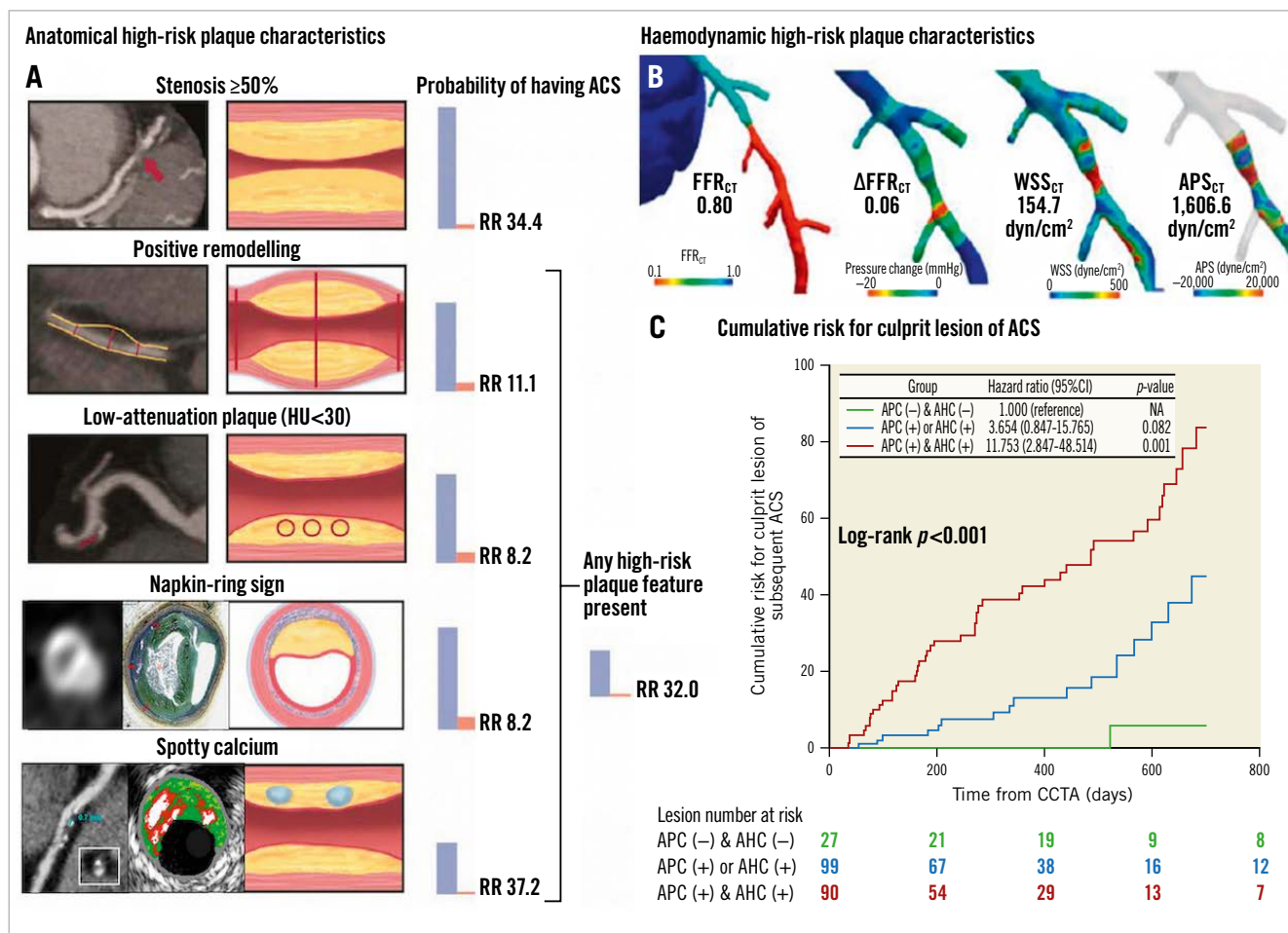
Figure 8. *Anatomical and haemodynamic plaque characteristics derived from CCTA. A) Probability of having ACS according to adverse plaque characteristics (APC). B) Adverse haemodynamic characteristics (AHC) based on 4 haemodynamic parameters derived from CCTA. C) Lesions with both APC and AHC showed significantly higher risk compared with those without. Reproduced/modified with permission from (A)[64], (B)[16], and (C)[72]. ACS: acute coronary syndrome; APS_{CT}: axial plaque stress derived from computed tomography; CCTA: coronary computed tomographic angiography; CI: confidence interval; FFR_{CT}: fractional flow reserve derived from coronary computed tomographic angiography; HU: Hounsfield units; RR: relative risk; WSS_{CT}: wall shear stress derived from computed tomography*

Recently, the APOLLO trial demonstrated that SLN360, a short interfering RNA (siRNA) targeting apo(a) production, reduced plasma Lp(a) concentrations in a dose-dependent manner[68]. If coronary plaque regression can be achieved in primary prevention and in patients with NOCAD by using subcutaneous injections of non-coding microRNA, with the findings confirmed by CCTA, then a similar pharmacology strategy should be rolled out and disseminated for secondary prevention in patients with much more advanced disease, pre- and post-revascularisation.

Even among plaques with the same vulnerable features, haemodynamic forces acting on the plaque can affect the risk of rupture since plaques can rupture when internal plaque stress exceeds plaque strength[72]. The EMERALD (Exploring the Mechanism of Plaque Rupture in Acute Coronary Syndrome Using Coronary CT Angiography and Computational Fluid Dynamic) study suggested that the ability to predict the risk of ACS, and thereby optimise treatment for those at high risk, could be enhanced by the integration of the four following non-invasive haemodynamic parameters derived from CCTA, (with cut-off values): 1) FFR_{CT} (0.80); 2) change in FFR_{CT} across the lesion (ΔFFR_{CT}, 0.06); 3) wall shear stress (154.7 dyn/cm^2); and 4) axial plaque stress (1,606.6 dyn/cm^2) **(Figure 8B, Figure 8C)**[72]. Anatomical and haemodynamic parameters derived from CCTA can help identify high-risk plaque, which can direct medical therapies.

RADIOMICS: DETECTION OF IMAGING BIOMARKERS BY AI
Quantitative imaging biomarkers that characterise tissue features – e.g., CAC (coronary artery calcium), LAP (low-attenuation plaque), FAI (fat attenuation index), and CMA (coronary microcalcification activity) – can be translated into histopathological concepts (e.g., LAP: lipid-rich plaque, necrotic core; FAI: inflamed perivascular fat), which can aid in the detection of vulnerable patients and provide objective decision-support tools in management pathways. In an era of machine learning and AI, it is

increasingly feasible to extract quantitative biomarkers from non-invasive images that go beyond plain radiological morphology but yield information on disease state and tissue characterisation. These can ultimately monitor the aggressiveness of disease and assess the response to treatment[73].

Radiomics, an emerging field in oncoradiology, is the process of extracting quantitative features from radiological examinations to create big data in order to identify novel imaging biomarkers not necessarily recognised by the human eye and brain but captured and classified by deep learning processes. Kolossváry et al demonstrated that CCTA-based radiomics has the potential to identify qualitative high-risk plaque features, e.g., napkin-ring sign, that, currently, only experts are capable of[74].

A prospective case-control study, including 60 patients with acute MI who underwent CCTA within 48 hours of admission and before ICA, compared the radiomic parameters of peri-coronary adipose tissue (PCAT) in patients with acute MI with those with stable or no CAD[75]. The results showed the most important radiomic parameters for distinguishing patients with or without MI were texture- (i.e., the spatial distribution of voxel grey-level intensities) and geometry- (i.e., shape, size, or volume) based parameters, providing information that was not captured by PCAT attenuation. These findings suggest that CCTA radiomics may become the next tool

for more precisely detecting imaging biomarkers and facilitating improved identification of vulnerable patients. There are admittedly many technical and post-processing challenges, including differences between machines, acquisition protocols, and reconstruction methods, that must be overcome before clinical application[76].

PCI PLANNING FOR FUNCTIONAL OBSTRUCTIVE CAD

CCTA as a "treatment planner" may facilitate, in advance or during percutaneous coronary intervention (PCI), the best fluoroscopic view with optimal exposure of the vessel to be treated (i.e., minimal foreshortening and overlap, maximal bifurcation angle), thereby reducing the number of exploratory injections of contrast medium and the amount of radiation needed to establish the optimal "working projection" for the procedure[77]. Kočka et al have designed a CCTA-based method to define optimal viewing angles of both coronary ostia and coronary bifurcation[78] **(Figure 9)**. Collet et al described the potential of the online real-time integration of 3D CCTA and fluoroscopic images in the catheterisation laboratory to improve PCI[77]. Planner projection of CCTA, with the option of longitudinal rotation and cross-sectional scrolling with instantaneous delineation of the vessel and lumen area along the vessel to be treated, enables vessel and lumen sizes, lesion length, calcium burden, and areas of low HU attenuation prone to
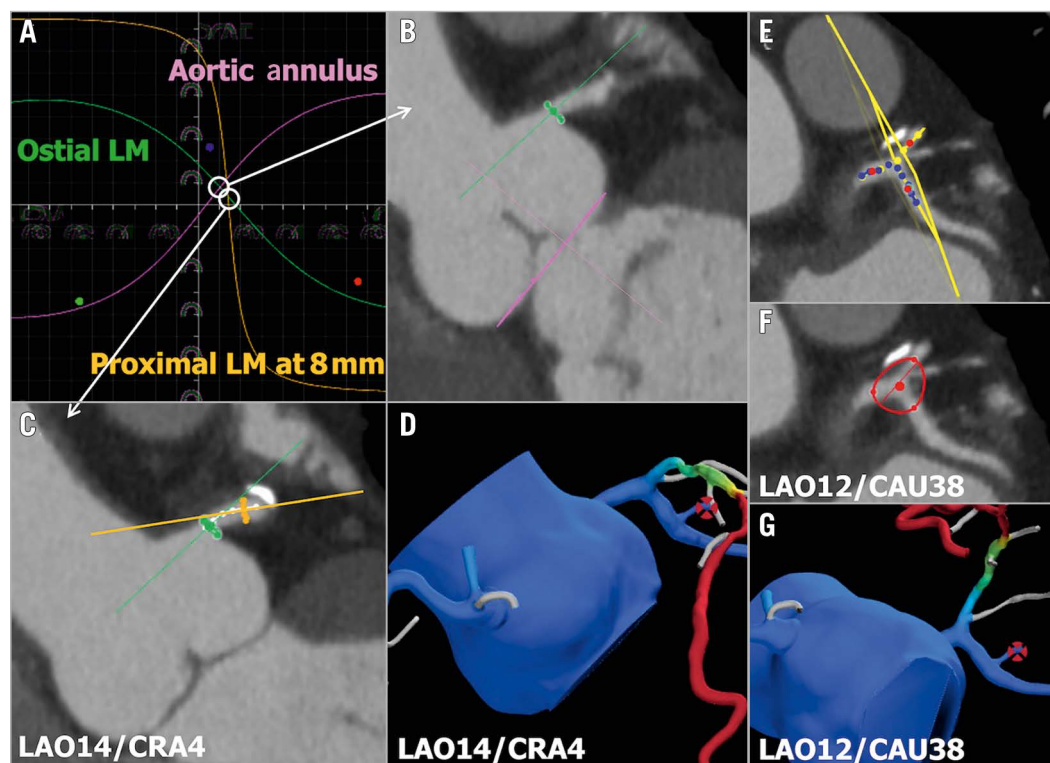
Figure 9. *Optimal fluoroscopic viewing angle for ostial, stem, and bifurcation of LM. A,B) The optimal fluoroscopic angle for ostial left main (LM) is obtained by the intersection between the aortic annulus and the ostial LM optimal projection curves. A,C) The optimal fluoroscopic angle for the LM stem is obtained by the intersection between the ostial LM and proximal LM optimal projection curves. D) FFR$_{CT}$ view matching the optimal angle of panel C. E,F) The optimal fluoroscopic angle for LM bifurcation is obtained as the perpendicular angle to the "en face" view created by placing 3 dots in the LM, left descending artery (LAD), and left circumflex artery (LCx) 5 mm from the point of the bifurcation. G) FFR$_{CT}$ view matching the optimal angle of panel F. FFR$_{CT}$: fractional flow reserve derived from coronary computed tomographic angiography*

generate periprocedural complications to be examined non-invasively and simultaneously displayed with the ICA on the fluoroscopic screen. This helps in the selection of devices to be used (e.g., drug-coated balloon, rotational atherectomy, or lithotripsy) as well as stent diameter and length[35] **(Supplementary Figure 7)**. Furthermore, during PCI, CCTA provides "live" IVUS-like imaging of the atherosclerotic plaque **(Supplementary Figure 6B, Supplementary Figure 6C)**. The optimisation of the angiographic information with plaque visualisation is likely to be translated into improved PCI techniques with complete plaque coverage, thereby improving clinical outcomes after PCI. This hypothesis is being tested in the ongoing P4 (Precise Procedural and PCI Plan; ClinicalTrials.gov: NCT05253677) randomised clinical trial comparing IVUS-guided PCI versus CT-guided PCI.

In a multicentre trial, randomising 400 patients with chronic total occlusions (CTO) to PCI with or without preprocedural CCTA, CTO PCI with CCTA guidance resulted in a higher success rate than those without (93.5% vs 84.0%; absolute difference 9.5%, 95% CI: 3.4-15.6%; p=0.003), which was attributed to the superior vessel tracking due to the greater understanding of the anatomical morphology of the occlusion from 3D information[79].

POST-PCI FFR AS PREDICTED FROM FFR$_{CT}$: THE "FFR$_{CT}$ PLANNER"

In focal, serial, or diffuse disease, a wire-based iFR/FFR pullback strategy in the catheterisation laboratory allows assessment after the initial stenting of the lesion(s). Residual significant pressure drop may guide the decision-making of subsequent stent placement in order to achieve post-PCI physiological values with favourable long-term prognosis[80]. The DEFINE PCI (Physiologic Assessment of Coronary Stenosis Following PCI) trial suggested that strategies based on this post-revascularisation physiology and completeness may help determine how to optimise revascularisation in individual patients[81]. The safety and effectiveness of this strategy to detect post-PCI ischaemia, normalise post-intervention physiology, and reduce clinical events will be prospectively evaluated in the DEFINE GPS (Distal Evaluation of Functional Performance With Intravascular Sensors to Assess the Narrowing Effect: Guided Physiologic Stenting; ClinicalTrials.gov: NCT04451044) trial. Furthermore, the advent of angiography-derived physiology provides post-PCI physiological assessment without the need for a pressure wire[82].

Although these pressure wire and invasive intracoronary imaging strategies aiming at optimisation of the procedure have the obvious advantage of repeated evaluation, virtual post-PCI FFR values can now be non-invasively computed from pre-PCI using the "FFR$_{CT}$ Planner" in the planning phase. The latter is a novel interactive tool for the prediction of post-PCI FFR through the virtual stenting of coronary stenoses. Recent data from the P3 (Precise Percutaneous Coronary Intervention Plan) study supports the high accuracy and precision of the FFR$_{CT}$ Planner for predicting invasive post-PCI FFR values[83]. These results were independent of CAD complexity (i.e., diffuse lesions, high calcium burden)

and image quality. The ability to predict post-PCI FFR might play an important role in patient selection and procedural planning, while achieving optimised post-PCI functional results, and, hence, improved outcomes.

DECISION-MAKING AND SURGICAL GUIDANCE IN PATIENTS WITH COMPLEX CAD

The SYNTAX (Synergy Between Percutaneous Coronary Intervention With TAXUS and Cardiac Surgery) III REVOLUTION trial demonstrated that clinical decision-making between coronary artery bypass graft (CABG) and PCI based on CCTA had a high agreement (concordance of decision 93% and Cohen's kappa 0.82) with the treatment decision derived from ICA in patients with 3VD with or without left main disease[2].

The ongoing FASTTRACK CABG (ClinicalTrials.gov: NCT04142021) trial evaluates the feasibility and the safety of planning and executing CABG based solely on CCTA combined with FFR$_{CT}$ without knowledge of the anatomy defined by ICA. The "CCTA Planning and Operating Heart Team" decides the surgical strategy guided by the anatomical and functional SYNTAX score provided by CCTA and FFR$_{CT}$ **(Figure 10)**. In addition, as a safety assessment, the residual anatomical and functional post-CABG SYNTAX score, based on 30-day CCTA, is calculated to evaluate the topographical adequacy of revascularisation with respect to surgical planning based on non-invasive imaging. In the future, it is plausible that CABG will be guided solely by non-invasive CCTA[84], although it will require high-quality CCTA images and interpreters, validated by the central core lab in the initial implementation.

Following confirmation by the surgeon that the most complex CAD can undergo CABG without access to conventional ICA, it becomes evident that the interventional cardiologist should have no reluctance in intervening in patients whose stenotic lesion's anatomy, functionality, and plaque composition are known by the operator in advance – even before entering the "catheterisation laboratory", now primarily used as an "interventional suite"[1].

EXTENDED REALITIES VISUALISATION DERIVED FROM CCTA AS A PREOPERATIVE PLANNING TOOL AND INTRAOPERATIVE SUPPORT

Spatial data visualisations (i.e., virtual or augmented reality) of 3D cardiac structures reconstructed from CCTA are expected, as pre- and peri-operative imaging tools more accurately facilitate the execution of surgical planning. Since operative planning requires spatial and 3D thinking that is not achievable on flat, 2D computer screens in conventional practice, Sadeghi et al implemented a technique of immersive 3D virtual reality for preoperative planning in six patients undergoing conventional or minimally invasive cardiac surgery[85].

Light objects called "holograms" derived from CCTA that are visualised using the mixed-reality technique (which allows an integration with the natural environment while maintaining direct interaction with both the digital and physical world) are expected
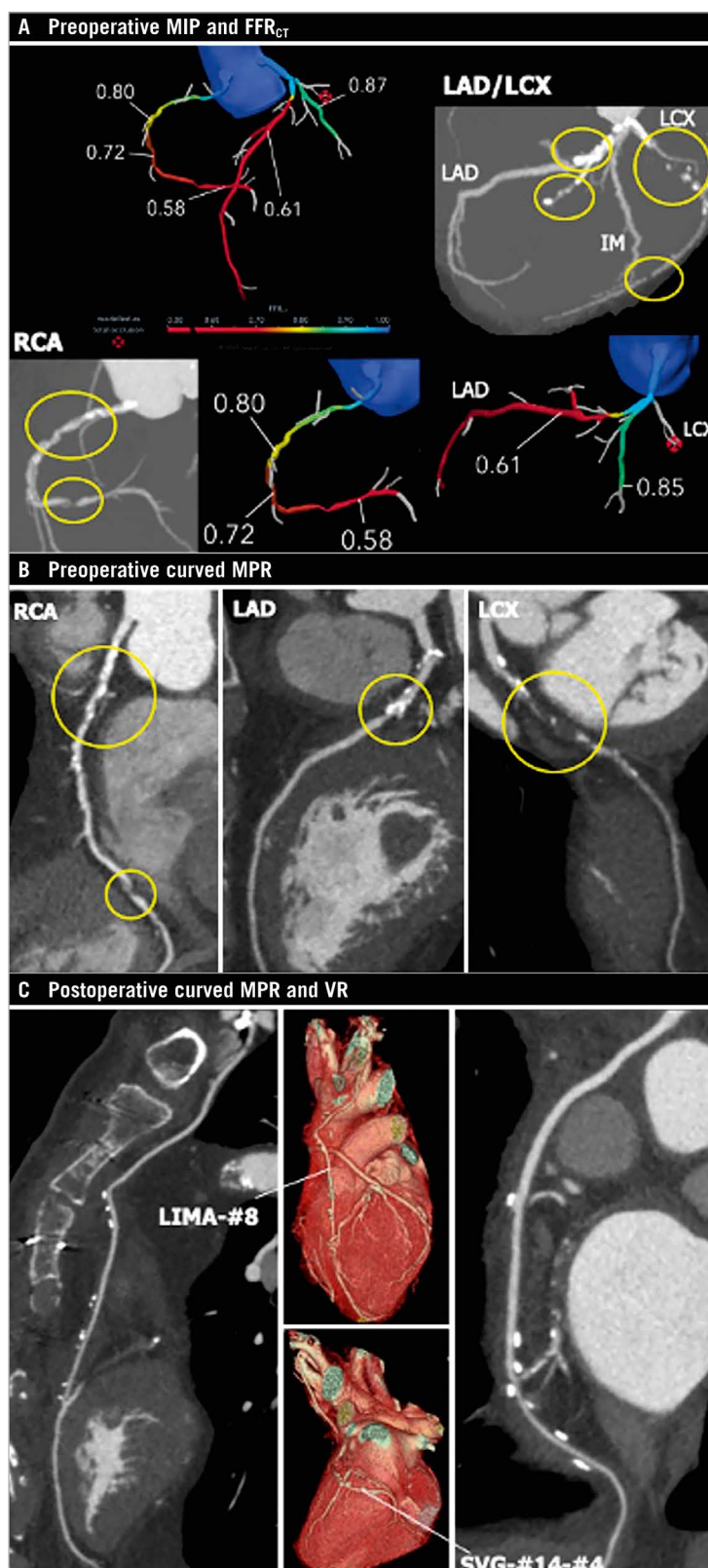
Figure 10. *Anatomical and physiological assessment based on non-invasive imaging for planning and follow-up of CABG. A) Preoperative maximum intensity projection (MIP) images and FFR_CT B) Preoperative curved multiplanar reconstruction (MPR) images: yellow circles indicate significant stenoses. FFR_CT indicates flow-limiting lesions at the proximal and distal RCA and proximal LAD, and total occlusion at the proximal LCx. C) Postoperative curved MPR and volume rendering (VR) images at 30-day follow-up. Left internal mammary artery (LIMA)-#8 and saphenous vein graft (SVG)-#14-#4 were patent. CABG: coronary artery bypass graft; FFR_CT: fractional flow reserve derived from coronary computed tomographic angiography; LAD: left anterior descending artery; LCx: left circumflex artery; RCA: right coronary artery*

to provide not only 3D surgical simulations during the planning phase, but also intraoperative support during CABG with real-world perception and touchless control **(Moving image 1, Moving image 2)**.

TECHNICAL FACTORS, OPTIMAL PRACTICAL PERFORMANCE, AND LIMITATIONS OF CCTA

The computation of FFR from CCTA requires coronary artery lumen segmentation methods to extract models from image data. This process is facilitated by subvoxel resolution techniques by which the spatial resolution of segmentation (approximately the size of a voxel: 0.25 mm) is able to exceed the voxel resolution (typically 0.5-0.7 mm) through subdividing the attenuation intensities within voxels and utilising machine learning to establish knowledge of the coronary artery lumen shapes and sizes across a large range of images and image features[86]. Thus, an assessment of the coronary artery geometry to generate a 3D finite element mesh can overcome the spatial resolution of the CCTA image.

Notably, in the PACIFIC trial, 83% of all vessels could be evaluated by FFR$_{CT}$. This drop-out rate suggested that optimal use of FFR$_{CT}$ in clinical practice greatly depends on high-quality images resulting from adequate pre-scan medication and low heart rates, as well as high-quality scanners, whereas MPI with SPECT/PET is usually not impeded by variable heart rates[27].

CCTA diagnostic reliability is highly dependent on image quality. Even when using the newest high-end scanners, it is vital to adhere to CCTA good practice guidelines. A target heart rate for CCTA set at less than 60 bpm is appropriate, but if it cannot be reached, scanning at a higher heart rate may be accepted, depending upon the scanner's temporal resolution[87]. Beta blockers are considered the first-line medication for achieving short-term heart rate reduction by oral, intravenous or both routes of drug administration. Nitroglycerin should be administered to achieve vasodilation and in order to improve the diagnostic accuracy of CCTA and stenosis assessment. With prospectively ECG-triggered axial acquisition, the X-ray tube is activated only during a prespecified phase of the cardiac cycle with no table motion during this time interval, saving in radiation exposure compared to retrospective ECG gain (up to 90%)[87]. The reconstruction kernel is the algorithm to compute the CT values for the pixel. "Soft" kernels produce an image of lower noise and lower spatial resolution, while "sharp" kernels increase resolution, reducing metal artefact or calcium blooming and increasing edge definition, at the cost of higher image noise.

Artefacts including calcification and motion affect CCTA interpretability. Blooming of metallic stent struts obscure up to 55% of the lumen within the stented segment, depending on strut thickness, image acquisition, and reconstruction parameters[25]. Since FFR$_{CT}$ requires accurate anatomical models, these artefacts may limit accuracy[88].

Plaque delineation and differentiation from the vessel wall and lumen on CCTA have not been achieved due to the limitations in the spatial resolution of current CT scanners, meaning that the vessel wall may be incorporated into non-calcified plaque volume[89]. In addition, increased density of adjacent calcified plaque may raise the density of contiguous low-attenuation high-risk plaque, due to the partial volume effect, leading to it being misclassified as fibrous plaque[89]. The plaque thresholds vary with lumen attenuation and reconstruction kernels. Currently no societal recommendation on how to identify plaques exist. Although promising outcome data are available, we have much more to learn for general utility in clinical practice.

Conclusions

Non-invasive coronary imaging by CCTA with functional assessment by FFR$_{CT}$ could become a cost-effective first-line patient pathway for the diagnosis of CAD. The adjunction of physiological epicardial conductance and myocardial resistance further boosts its diagnostic capacity. Decision-making between pharmacological treatment, PCI, and CABG based solely on non-invasive imaging may become a reality. NOCAD can be diagnosed by non-invasive imaging and become a privileged target for primary prevention based on lifestyle modification with/without aggressive pharmacological treatment.

Appendix. Authors' affiliations

1. Department of Cardiology, University of Galway, Galway, Ireland; 2. Department of Cardiology, Aarhus University Hospital, Aarhus, Denmark; 3. Department of Cardiology, Royal Blackburn Hospital, Blackburn, UK; 4. Department of Radiology and Division of Cardiovascular Medicine, Stanford University School of Medicine, Palo Alto, CA, USA; 5. Centre for Cardiovascular Science, University of Edinburgh, Edinburgh, UK; 6. Department of Cardiology, Leiden University Medical Center, Leiden, the Netherlands; 7. Heart Center, Turku University Hospital and University of Turku, Turku, Finland; 8. Mount Sinai Medical Center, New York, NY, USA; 9. School of Cardiovascular Medicine and Sciences, British Heart Foundation Centre of Research Excellence, King's College London, London, UK; 10. HeartFlow, Inc., Redwood City, CA, USA; 11. Department of Medicine and Radiology, University of British Columbia, Vancouver, British Columbia, Canada; 12. Royal Brompton Hospital, London, UK; 13. School of Biomedical Engineering and Imaging Sciences, King's College London, London, UK; 14. Department of Medicine, Division of Cardiology, McGill University Health Center, Montreal, Quebec, Canada; 15. Division of Internal Medicine, Medical School, University of Western Australia, Perth, WA, Australia; 16. Department of Cardiology, Royal Perth Hospital, Perth, WA, Australia; 17. Department of Advanced Diagnostic Imaging, Mie University Graduate School of Medicine, Mie, Japan; 18. Cardiovascular Center Aalst, OLV-Clinic, Aalst, Belgium; 19. Department of Cardiology, Lausanne University Hospital (CHUV), Lausanne, Switzerland; 20. Department of Radiology, Universitair Ziekenhuis Brussel, VUB, Brussels,

Belgium; 21. Centro Cardiologico Monzino, IRCCS, Milan, Italy; 22. Szpital Uniwersytecki w Krakowie, Krakow, Poland; 23. Digital Innovations & Robotics Hub, Krakow, Poland; 24. Department of Measurement and Electronics, AGH University of Science and Technology, Krakow, Poland; 25. School of Biomedical Engineering, Shanghai Jiao Tong University, Shanghai, People's Republic of China; 26. The Lambe Institute for Translational Medicine, The Smart Sensors Laboratory and CURAM, Galway, University of Galway, Galway, Ireland; 27. Division of Cardiology, Harbor-UCLA Medical Center, Torrance, CA, USA; 28. Division of Cardiology and Cardiac Imaging, IRCCS Galeazzi Sant'Ambrogio, Milan, Italy; 29. Department of Biomedical and Clinical Sciences, University of Milan, Milan, Italy.

Conflict of interest statement

References

1. Serruys PW, Hara H, Garg S, Kawashima H, Nørgaard BL, Dweck MR, Bax JJ, Knuuti J, Nieman K, Leipsic JA, Mushtaq S, Andreini D, Onuma Y. Coronary Computed Tomographic Angiography for Complete Assessment of Coronary Artery Disease: JACC State-of-the-Art Review. *J Am Coll Cardiol.* 2021;78:713-36.

2. Collet C, Onuma Y, Andreini D, Sonck J, Pompilio G, Mushtaq S, La Meir M, Miyazaki Y, de Mey J, Gaemperli O, Ouda A, Maureira JP, Mandry D, Camenzind E, Macron L, Doenst T, Teichgräber U, Sigusch H, Asano T, Katagiri Y, Morel MA, Lindeboom W, Pontone G, Lüscher TF, Bartorelli AL, Serruys PW. Coronary computed tomography angiography for heart team decision-making in multivessel coronary artery disease. *Eur Heart J.* 2018;39:3689-98.

3. Serruys PW, Chichareon P, Modolo R, Leaman DM, Reiber JHC, Emanuelsson H, Di Mario C, Pijls NHJ, Morel MA, Valgimigli M, Farooq V, van Klaveren D, Capodanno D, Andreini D, Bourantas CV, Davies J, Banning AP, Escaned J, Piek JJ, Echavarría-Pinto M, Taylor CA, Thomsen B, Collet C, Pompilio G, Bartorelli AL, Glocker B, Dressler O, Stone GW, Onuma Y. The SYNTAX score on its way out or … towards artificial intelligence: part II. *EuroIntervention.* 2020;16:60-75.

4. Kunadian V, Chieffo A, Camici PG, Berry C, Escaned J, Maas AHEM, Prescott E, Karam N, Appelman Y, Fraccaro C, Louise Buchanan G, Manzo-Silberman S, Al-Lamee R, Regar E, Lansky A, Abbott JD, Badimon L, Duncker DJ, Mehran R, Capodanno D, Baumbach A. An EAPCI Expert Consensus Document on Ischaemia with Non-Obstructive Coronary Arteries in Collaboration with European Society of Cardiology Working Group on Coronary Pathophysiology & Microcirculation Endorsed by Coronary Vasomotor Disorders International Study Group. *Eur Heart J.* 2020;41:3504-20.

5. Knuuti J, Wijns W, Saraste A, Capodanno D, Barbato E, Funck-Brentano C, Prescott E, Storey RF, Deaton C, Cuisset T, Agewall S, Dickstein K, Edvardsen T, Escaned J, Gersh BJ, Svitil P, Gilard M, Hasdai D, Hatala R, Mahfoud F, Masip J, Muneretto C, Valgimigli M, Achenbach S, Bax JJ; ESC Scientific Document Group. 2019 ESC Guidelines for the diagnosis and management of chronic coronary syndromes. *Eur Heart J.* 2020;41:407-77.

6. Foldyna B, Udelson JE, Karády J, Banerji D, Lu MT, Mayrhofer T, Bittner DO, Meyersohn NM, Emami H, Genders TSS, Fordyce CB, Ferencik M, Douglas PS, Hoffmann U. Pretest probability for patients with suspected obstructive coronary artery disease: re-evaluating Diamond-Forrester for the contemporary era and clinical implications: insights from the PROMISE trial. *Eur Heart J Cardiovasc Imaging.* 2019;20:574-81.

7. Bing R, Singh T, Dweck MR, Mills NL, Williams MC, Adamson PD, Newby DE. Validation of European Society of Cardiology pre-test probabilities for obstructive coronary artery disease in suspected stable angina. *Eur Heart J Qual Care Clin Outcomes.* 2020;6:293-300.

8. Mortensen MB, Dzaye O, Steffensen FH, Bøtker HE, Jensen JM, Rønnow Sand NP, Kragholm KH, Sørensen HT, Leipsic J, Mæng M, Blaha MJ, Nørgaard BL. Impact of Plaque Burden Versus Stenosis on Ischemic Events in Patients With Coronary Atherosclerosis. *J Am Coll Cardiol.* 2020;76:2803-13.

9. Writing Committee Members, Gulati M, Levy PD, Mukherjee D, Amsterdam E, Bhatt DL, Birtcher KK, Blankstein R, Boyd J, Bullock-Palmer RP, Conejo T, Diercks DB, Gentile F, Greenwood JP, Hess EP, Hollenberg SM, Jaber WA, Jneid H, Joglar JA, Morrow DA, O'Connor RE, Ross MA, Shaw LJ. 2021 AHA/ACC/ASE/CHEST/SAEM/SCCT/SCMR Guideline for the Evaluation and Diagnosis of Chest Pain: A Report of the American College of Cardiology/American Heart Association Joint Committee on Clinical Practice Guidelines. *J Am Coll Cardiol.* 2021;78:e187-285.

10. Cury RC, Blankstein R, Leipsic J, Abbara S, Achenbach S, Berman D, Bittencourt M, Budoff M, Chinnaiyan K, Choi AD, Ghoshhajra B, Jacobs J, Koweek L, Lesser J, Maroules C, Rubin GD, Rybicki FJ, Shaw LJ, Williams MC, Williamson E, White CS, Villines TC. CAD-RADS™ 2.0 - 2022 Coronary Artery Disease - Reporting and Data System an expert consensus document of the Society of Cardiovascular Computed Tomography (SCCT), the American College of Cardiology (ACC), the American College of Radiology (ACR) and the North America society of cardiovascular imaging (NASCI). *J Cardiovasc Comput Tomogr.* 2022;16:536-57.

11. Xie JX, Cury RC, Leipsic J, Crim MT, Berman DS, Gransar H, Budoff MJ, Achenbach S, Ó Hartaigh B, Callister TQ, Marques H, Rubinshtein R, Al-Mallah MH, Andreini D, Pontone G, Cademartiri F, Maffei E, Chinnaiyan K, Raff G, Hadamitzky M, Hausleiter J, Feuchtner G, Dunning A, DeLago A, Kim YJ, Kaufmann PA, Villines TC, Chow BJW, Hindoyan N, Gomez M, Lin FY, Jones E, Min JK, Shaw LJ. The Coronary Artery Disease–Reporting and Data System (CAD-RADS): Prognostic and Clinical Implications Associated With Standardized Coronary Computed Tomography Angiography Reporting. *JACC Cardiovasc Imaging.* 2018;11:78-89.

12. Hecht HS, Blaha MJ, Kazerooni EA, Cury RC, Budoff M, Leipsic J, Shaw L. CAC-DRS: Coronary Artery Calcium Data and Reporting System. An expert consensus document of the Society of Cardiovascular Computed Tomography (SCCT). *J Cardiovasc Comput Tomogr.* 2018;12:185-91.

13. Williams MC, Moss A, Dweck M, Hunter A, Pawade T, Adamson PD, Shah ASV, Alam S, Maroules CD, van Beek EJ, Cury R, Nicol ED, Newby DE, Roditi G. Standardized reporting systems for computed tomography coronary angiography and calcium scoring: A real-world validation of CAD-RADS and CAC-DRS in patients with stable chest pain. *J Cardiovasc Comput Tomogr.* 2020;14:3-11.

14. Knuuti J, Ballo H, Juarez-Orozco LE, Saraste A, Kolh P, Rutjes AWS, Jüni P, Windecker S, Bax JJ, Wijns W. The performance of non-invasive tests to rule-in and rule-out significant coronary artery stenosis in patients with stable angina: a meta-analysis focused on post-test disease probability. *Eur Heart J.* 2018;39:3322-30.

15. Latina J, Shabani M, Kapoor K, Whelton SP, Trost JC, Sesso J, Demehri S, Mahesh M, Lima JAC, Arbab-Zadeh A. Ultra-High-Resolution Coronary CT Angiography for Assessment of Patients with Severe Coronary Artery Calcification: Initial Experience. *Radiol Cardiothorac Imaging.* 2021;3:e210053.

16. Nicol ED, Norgaard BL, Blanke P, Ahmadi A, Weir-McCall J, Horvat PM, Han K, Bax JJ, Leipsic J. The Future of Cardiovascular Computed Tomography: Advanced Analytics and Clinical Insights. *JACC Cardiovasc Imaging.* 2019;12:1058-72.

17. Kwan AC, Pourmorteza A, Stutman D, Bluemke DA, Lima JAC. Next-Generation Hardware Advances in CT: Cardiac Applications. *Radiology.* 2021;298:3-17.

18. Schuijf JD, Lima JAC, Boedeker KL, Takagi H, Tanaka R, Yoshioka K, Arbab-Zadeh A. CT imaging with ultra-high-resolution: Opportunities for cardiovascular imaging in clinical practice. *J Cardiovasc Comput Tomogr.* 2022;16:388-96

19. Griffin WF, Choi AD, Riess JS, Marques H, Chang HJ, Choi JH, Doh JH, Her AY, Koo BK, Nam CW, Park HB, Shin SH, Cole J, Gimelli A, Khan MA, Lu B, Gao Y, Nabi F, Nakazato R, Schoepf UJ, Driessen RS, Bom MJ, Thompson R, Jang JJ, Ridner M, Rowan C, Avelar E, Généreux P, Knaapen P, de Waard GA, Pontone G, Andreini D, Earls JP. AI Evaluation of Stenosis on Coronary CT Angiography, Comparison With Quantitative Coronary Angiography and Fractional Flow Reserve: A CREDENCE Trial Substudy. *JACC Cardiovasc Imaging.* 2023;16:193-205.

20. Lu MT, Meyersohn NM, Mayrhofer T, Bittner DO, Emami H, Puchner SB, Foldyna B, Mueller ME, Hearne S, Yang C, Achenbach S, Truong QA, Ghoshhajra BB, Patel MR, Ferencik M, Douglas PS, Hoffmann U. Central Core Laboratory versus Site Interpretation of Coronary CT Angiography: Agreement and Association with Cardiovascular Events in the PROMISE Trial. *Radiology.* 2017;287:87-95.

21. Lin A, Manral N, McElhinney P, Killekar A, Matsumoto H, Kwiecinski J, Pieszko K, Razipour A, Grodecki K, Park C, Otaki Y, Doris M, Kwan AC, Han D, Kuronuma K, Flores Tomasino G, Tzolos E, Shanbhag A, Goeller M, Marwan M, Gransar H, Tamarappoo BK, Cadet S, Achenbach S, Nicholls SJ, Wong DT, Berman DS, Dweck M, Newby DE, Williams MC, Slomka PJ, Dey D. Deep learning-enabled coronary CT angiography for plaque and stenosis quantification and cardiac risk prediction: an international multicentre study. *Lancet Digit Health.* 2022;4:e256-65.

22. Lee KK, Bularga A, O'Brien R, Ferry AV, Doudesis D, Fujisawa T, Kelly S, Stewart S, Wereski R, Cranley D, van Beek EJR, Lowe DJ, Newby DE, Williams MC, Gray AJ, Mills NL. Troponin-Guided Coronary Computed Tomographic Angiography After Exclusion of Myocardial Infarction. *J Am Coll Cardiol.* 2021;78:1407-17.

23. SCOT-HEART Investigators, Newby DE, Adamson PD, Berry C, Boon NA, Dweck MR, Flather M, Forbes J, Hunter A, Lewis S, MacLean S, Mills NL, Norrie J, Roditi G, Shah ASV, Timmis AD, van Beek EJR, Williams MC. Coronary CT Angiography and 5-Year Risk of Myocardial Infarction. *N Engl J Med.* 2018;379:924-33.

24. Ferencik M, Mayrhofer T, Bittner DO, Emami H, Puchner SB, Lu MT, Meyersohn NM, Ivanov AV, Adami EC, Patel MR, Mark DB, Udelson JE, Lee KL, Douglas PS, Hoffmann U. Use of High-Risk Coronary Atherosclerotic Plaque Detection for Risk Stratification of Patients With Stable Chest Pain: A Secondary Analysis of the PROMISE Randomized Clinical Trial. *JAMA Cardiology.* 2018;3:144-52.

25. Narula J, Chandrashekhar Y, Ahmadi A, Abbara S, Berman DS, Blankstein R, Leipsic J, Newby D, Nicol ED, Nieman K, Shaw L, Villines TC, Williams M, Hecht HS. SCCT 2021 Expert Consensus Document on Coronary Computed Tomographic Angiography: A Report of the Society of Cardiovascular Computed Tomography. *J Cardiovasc Comput Tomogr.* 2021;15:192-217.

26. Nørgaard BL, Sand NP, Jensen JM. Is CT-derived fractional flow reserve superior to ischemia testing? *Expert Rev Cardiovasc Ther.* 2022;20:165-8.

27. Driessen RS, Danad I, Stuijfzand WJ, Raijmakers PG, Schumacher SP, van Diemen PA, Leipsic JA, Knuuti J, Underwood SR, van de Ven PM, van Rossum AC, Taylor CA, Knaapen P. Comparison of Coronary Computed Tomography Angiography, Fractional Flow Reserve, and Perfusion Imaging for Ischemia Diagnosis. *J Am Coll Cardiol.* 2019;73:161-73.

28. Rasmussen LD, Winther S, Westra J, Isaksen C, Ejlersen JA, Brix L, Kirk J, Urbonaviciene G, Søndergaard HM, Hammid O, Schmidt SE, Knudsen LL, Madsen LH, Frost L, Petersen SE, Gormsen LC, Christiansen EH, Eftekhari A, Holm NR, Nyegaard M, Chiribiri A, Bøtker HE, Böttcher M. Danish study of Non-Invasive testing in Coronary Artery Disease 2 (Dan-NICAD 2): Study design for a controlled study of diagnostic accuracy. *Am Heart J.* 2019;215:114-28.

29. Curzen N, Nicholas Z, Stuart B, Wilding S, Hill K, Shambrook J, Eminton Z, Ball D, Barrett C, Johnson L, Nuttall J, Fox K, Connolly D, O'Kane P, Hobson A, Chauhan A, Uren N, Mccann G, Berry C, Carter J, Roobottom C, Mamas M, Rajani R, Ford I, Douglas P, Hlatky M. Fractional flow reserve derived from computed tomography coronary angiography in the assessment and management of stable chest pain: the FORECAST randomized trial. *Eur Heart J.* 2021;42:3844-52.

30. Pontone G, Rossi A, Guglielmo M, Dweck MR, Gaemperli O, Nieman K, Pugliese F, Maurovich-Horvat P, Gimelli A, Cosyns B, Achenbach S. Clinical applications of cardiac computed tomography: a consensus paper of the European Association of Cardiovascular Imaging-part II. *Eur Heart J Cardiovasc Imaging.* 2022;23:e136-61.

31. Patel MR, Nørgaard BL, Fairbairn TA, Nieman K, Akasaka T, Berman DS, Raff GL, Hurwitz Koweek LM, Pontone G, Kawasaki T, Sand NPR, Jensen JM, Amano T, Poon M, Øvrehus KA, Sonck J, Rabbat MG, Mullen S, De Bruyne B, Rogers C, Matsuo H, Bax JJ, Leipsic J. 1-Year Impact on Medical Practice and Clinical Outcomes of FFR$_{CT}$: The ADVANCE Registry. *JACC Cardiovasc Imaging.* 2020;13:97-105.

32. Nørgaard BL, Gaur S, Fairbairn TA, Douglas PS, Jensen JM, Patel MR, Ihdayhid AR, Ko BSH, Sellers SL, Weir-McCall J, Matsuo H, Sand NPR, Øvrehus KA, Rogers C, Mullen S, Nieman K, Parner E, Leipsic J, Abdulla J. Prognostic value of coronary computed tomography angiographic derived fractional flow reserve: a systematic review and meta-analysis. *Heart.* 2022;108:194-202.

33. Ihdayhid AR, Norgaard BL, Gaur S, Leipsic J, Nerlekar N, Osawa K, Miyoshi T, Jensen JM, Kimura T, Shiomi H, Erglis A, Jegere S, Oldroyd KG, Botker HE, Seneviratne SK, Achenbach S, Ko BS. Prognostic Value and Risk Continuum of Noninvasive Fractional Flow Reserve Derived from Coronary CT Angiography. *Radiology.* 2019;292:343-51.

34. Schoepf UJ, van Assen M. FFR-CT and CT Myocardial Perfusion Imaging: Friends or Foes? *JACC Cardiovasc Imaging.* 2019;12:2472-4.

35. Andreini D, Collet C, Leipsic J, Nieman K, Bittencurt M, De Mey J, Buls N, Onuma Y, Mushtaq S, Conte E, Bartorelli AL, Stefanini G, Sonck J, Knaapen P, Ghoshhajra B, Serruys PW. Pre-procedural Planning of Coronary Revascularization by Cardiac Computed Tomography : An Expert Consensus Document of the Society of Cardiovascular Computed Tomography. *EuroIntervention.* 2022;18:e872-7

36. Celeng C, Leiner T, Maurovich-Horvat P, Merkely B, de Jong P, Dankbaar JW, van Es HW, Ghoshhajra BB, Hoffmann U, Takx RAP. Anatomical and Functional Computed Tomography for Diagnosing Hemodynamically Significant Coronary Artery Disease: A Meta-Analysis. *JACC Cardiovasc Imaging.* 2019;12:1316-25.

37. Patel AR, Bamberg F, Branch K, Carrascosa P, Chen M, Cury RC, Ghoshhajra B, Ko B, Nieman K, Pugliese F, Schoepf J, Blankstein R. Society of cardiovascular computed tomography expert consensus document on myocardial computed tomography perfusion imaging. *J Cardiovasc Comput Tomogr.* 2020;14:87-100.

38. Danad I, Szymonifka J, Schulman-Marcus J, Min JK. Static and dynamic assessment of myocardial perfusion by computed tomography. *Eur Heart J Cardiovasc Imaging.* 2016;17:836-44.

39. Pontone G, Baggiano A, Andreini D, Guaricci AI, Guglielmo M, Muscogiuri G, Fusini L, Fazzari F, Mushtaq S, Conte E, Calligaris G, De Martini S, Ferrari C, Galli S, Grancini L, Ravagnani P, Teruzzi G, Trabattoni D, Fabbiocchi F, Lualdi A, Montorsi P, Rabbat MG, Bartorelli AL, Pepi M. Stress Computed Tomography Perfusion Versus Fractional Flow Reserve CT Derived in Suspected Coronary Artery Disease: The PERFECTION Study. *JACC Cardiovasc Imaging.* 2019;12:1487-97.

40. Dewey M, Rochitte CE, Ostovaneh MR, Chen MY, George RT, Niinuma H, Kitagawa K, Laham R, Kofoed K, Nomura C, Sakuma H, Yoshioka K, Mehra VC, Jinzaki M, Kuribayashi S, Laule M, Paul N, Scholte AJ, Cerci R, Hoe J, Tan SY, Rybicki FJ, Matheson MB, Vavere AL, Arai AE, Miller JM, Cox C, Brinker J, Clouse ME, Di Carli M, Lima JAC, Arbab-Zadeh A. Prognostic value of noninvasive combined anatomic/functional assessment by cardiac CT in patients with suspected coronary artery disease - Comparison with invasive coronary angiography and nuclear myocardial perfusion imaging for the five-year-follow up of the CORE320 multicenter study. *J Cardiovasc Comput Tomogr.* 2021;15:485-91.

41. Kitagawa K, Nakamura S, Ota H, Ogawa R, Shizuka T, Kubo T, Yi Y, Ito T, Nagasawa N, Omori T, Nakamori S, Kurita T, Sugisawa J, Hatori N, Nakashima H, Wang Y, Kido T, Watanabe K, Matsumoto Y, Dohi K, Sakuma H. Diagnostic Performance of Dynamic Myocardial Perfusion Imaging Using Dual-Source Computed Tomography. *J Am Coll Cardiol.* 2021;78:1937-49.

42. Nous FMA, Geisler T, Kruk MBP, Alkadhi H, Kitagawa K, Vliegenthart R, Hell MM, Hausleiter J, Nguyen PK, Budde RPJ, Nikolaou K, Kepka C, Manka R, Sakuma H, Malik SB, Coenen A, Zijlstra F, Klotz E, van der Harst P, Artzner C, Dedic A, Pugliese F, Bamberg F, Nieman K. Dynamic Myocardial Perfusion CT for the Detection of Hemodynamically Significant Coronary Artery Disease. *JACC Cardiovasc Imaging.* 2022;15:75-87.

43. Lubbers M, Coenen A, Kofflard M, Bruning T, Kietselaer B, Galema T, Kock M, Niezen A, Das M, van Gent M, van den Bos EJ, van Woerkens L, Musters P, Kooij S, Nous F, Budde R, Hunink M, Nieman K. Comprehensive Cardiac CT With Myocardial Perfusion Imaging Versus Functional Testing in Suspected Coronary Artery Disease: The Multicenter, Randomized CRESCENT-II Trial. *JACC Cardiovasc Imaging.* 2018;11:1625-36.

44. Ihdayhid AR, Fairbairn TA, Gulsin GS, Tzimas G, Danehy E, Updegrove A, Jensen JM, Taylor CA, Bax JJ, Sellers SL, Leipsic JA, Nørgaard BL. Cardiac computed tomography-derived coronary artery volume to myocardial mass. *J Cardiovasc Comput Tomogr.* 2022;16:198-206.

45. Taylor CA, Gaur S, Leipsic J, Achenbach S, Berman DS, Jensen JM, Dey D, Bøtker HE, Kim HJ, Khem S, Wilk A, Zarins CK, Bezerra H, Lesser J, Ko B, Narula J, Ahmadi A, Øvrehus KA, St Goar F, De Bruyne B, Nørgaard BL. Effect of the ratio of coronary arterial lumen volume to left ventricle myocardial mass derived from coronary CT angiography on fractional flow reserve. *J Cardiovasc Comput Tomogr.* 2017;11:429-36.

46. van Diemen PA, Schumacher SP, Bom MJ, Driessen RS, Everaars H, Stuijfzand WJ, Raijmakers PG, van de Ven PM, Min JK, Leipsic JA, Knuuti J, Boellaard PR, Taylor CA, van Rossum AC, Danad I, Knaapen P. The association of coronary lumen volume to left ventricle mass ratio with myocardial blood flow and fractional flow reserve. *J Cardiovasc Comput Tomogr.* 2019;13:179-87.

47. Kogame N, Ono M, Kawashima H, Tomaniak M, Hara H, Leipsic J, Andreini D, Collet C, Patel MR, Tu S, Xu B, Bourantas CV, Lerman A, Piek JJ, Davies JE, Escaned J, Wijns W, Onuma Y, Serruys PW. The Impact of Coronary Physiology on Contemporary Clinical Decision Making. *JACC Cardiovasc Interv.* 2020;13:1617-38.

48. Taqueti VR, Di Carli MF. Coronary Microvascular Disease Pathogenic Mechanisms and Therapeutic Options: JACC State-of-the-Art Review. *J Am Coll Cardiol.* 2018;72:2625-41.

49. Jaquet C, Najman L, Talbot H, Grady L, Schaap M, Spain B, Kim HJ, Vignon-Clementel I, Taylor CA. Generation of Patient-Specific Cardiac Vascular Networks: A Hybrid Image-Based and Synthetic Geometric Model. *IEEE Trans Biomed Eng.* 2019;66:946-55.

50. Papamanolis L, Kim HJ, Jaquet C, Sinclair M, Schaap M, Danad I, van Diemen P, Knaapen P, Najman L, Talbot H, Taylor CA, Vignon-Clementel I. Myocardial Perfusion Simulation for Coronary Artery Disease: A Coupled Patient-Specific Multiscale Model. *Ann Biomed Eng.* 2021;49:1432-47.

51. Arnett DK, Blumenthal RS, Albert MA, Buroker AB, Goldberger ZD, Hahn EJ, Himmelfarb CD, Khera A, Lloyd-Jones D, McEvoy JW, Michos ED, Miedema MD, Muñoz D, Smith SC Jr, Virani SS, Williams KA Sr, Yeboah J, Ziaeian B. 2019 ACC/AHA Guideline on the Primary Prevention of Cardiovascular Disease: A Report of the American College of Cardiology/American Heart Association Task Force on Clinical Practice Guidelines. *Circulation.* 2019;140:e596-646.

52. Dawson LP, Lum M, Nerleker N, Nicholls SJ, Layland J. Coronary Atherosclerotic Plaque Regression: JACC State-of-the-Art Review. *J Am Coll Cardiol.* 2022;79:66-82.

53. Bergström G, Persson M, Adiels M, Björnson E, Bonander C, Ahlström H, Alfredsson J, Angerås O, Berglund G, Blomberg A, Brandberg J, Börjesson M, Cederlund K, Faire Ud, Duvernoy O, Ekblom Ö, Engström G, Engvall JE, Fagman E, Eriksson M, Erlinge D, Fagerberg B, Flinck A, Gonçalves I, Hagström E, Hjelmgren O, Lind L, Lindberg E, Lindqvist P, Ljungberg J, Magnusson M, Mannila M, Markstad H, Mohammad MA, Nystrom FH, Ostenfeld E, Persson A, Rosengren A, Sandström A, Själander A, Sköld MC, Sundström J, Swahn E, Söderberg S, Torén K, Östgren CJ,

Jernberg T. Prevalence of Subclinical Coronary Artery Atherosclerosis in the General Population. *Circulation.* 2021;144:916-29.

54. Mushtaq S, De Araujo Gonçalves P, Garcia-Garcia HM, Pontone G, Bartorelli AL, Bertella E, Campos CM, Pepi M, Serruys PW, Andreini D. Long-term prognostic effect of coronary atherosclerotic burden: validation of the computed tomography-Leaman score. *Circ Cardiovasc Imaging.* 2015;8:e002332.

55. Andreini D, Pontone G, Mushtaq S, Gransar H, Conte E, Bartorelli AL, Pepi M, Opolski MP, Ó Hartaigh B, Berman DS, Budoff MJ, Achenbach S, Al-Mallah M, Cademartiri F, Callister TQ, Chang HJ, Chinnaiyan K, Chow BJ, Cury R, Delago A, Hadamitzky M, Hausleiter J, Feuchtner G, Kim YJ, Kaufmann PA, Leipsic J, Lin FY, Maffei E, Raff G, Shaw LJ, Villines TC, Dunning A, Marques H, Rubinshtein R, Hindoyan N, Gomez M, Min JK. Long-term prognostic impact of CT-Leaman score in patients with non-obstructive CAD: Results from the COronary CT Angiography EvaluatioN For Clinical Outcomes InteRnational Multicenter (CONFIRM) study. *Int J Cardiol.* 2017;231:18-25.

56. van Rosendael AR, Shaw LJ, Xie JX, Dimitriu-Leen AC, Smit JM, Scholte AJ, van Werkhoven JM, Callister TQ, DeLago A, Berman DS, Hadamitzky M, Hausleiter J, Al-Mallah MH, Budoff MJ, Kaufmann PA, Raff G, Chinnaiyan K, Cademartiri F, Maffei E, Villines TC, Kim YJ, Feuchtner G, Lin FY, Jones EC, Pontone G, Andreini D, Marques H, Rubinshtein R, Achenbach S, Dunning A, Gomez M, Hindoyan N, Gransar H, Leipsic J, Narula J, Min JK, Bax JJ. Superior Risk Stratification With Coronary Computed Tomography Angiography Using a Comprehensive Atherosclerotic Risk Score. *JACC Cardiovasc Imaging.* 2019;12:1987-97.

57. Oikonomou EK, Marwan M, Desai MY, Mancio J, Alashi A, Hutt Centeno E, Thomas S, Herdman L, Kotanidis CP, Thomas KE, Griffin BP, Flamm SD, Antonopoulos AS, Shirodaria C, Sabharwal N, Deanfield J, Neubauer S, Hopewell JC, Channon KM, Achenbach S, Antoniades C. Non-invasive detection of coronary inflammation using computed tomography and prediction of residual cardiovascular risk (the CRISP CT study): a post-hoc analysis of prospective outcome data. *Lancet.* 2018;392:929-39.

58. Kwiecinski J, Tzolos E, Adamson PD, Cadet S, Moss AJ, Joshi N, Williams MC, van Beek EJR, Dey D, Berman DS, Newby DE, Slomka PJ, Dweck MR. Coronary ¹⁸F-Sodium Fluoride Uptake Predicts Outcomes in Patients With Coronary Artery Disease. *J Am Coll Cardiol.* 2020;75:3061-74.

59. Tarkin JM, Joshi FR, Evans NR, Chowdhury MM, Figg NL, Shah AV, Starks LT, Martin-Garrido A, Manavaki R, Yu E, Kuc RE, Grassi L, Kreuzhuber R, Kostadima MA, Frontini M, Kirkpatrick PJ, Coughlin PA, Gopalan D, Fryer TD, Buscombe JR, Groves AM, Ouwehand WH, Bennett MR, Warburton EA, Davenport AP, Rudd JH. Detection of Atherosclerotic Inflammation by ⁶⁸Ga-DOTATATE PET Compared to [¹⁸F]FDG PET Imaging. *J Am Coll Cardiol.* 2017;69:1774-91.

60. Conte E, Mushtaq S, Pontone G, Li Piani L, Ravagnani P, Galli S, Collet C, Sonck J, Di Odoardo L, Guglielmo M, Baggiano A, Trabattoni D, Annoni A, Mancini ME, Formenti A, Muscogiuri G, Magatelli M, Nicoli F, Poggi C, Fiorentini C, Bartorelli AL, Pepi M, Montorsi P, Andreini D. Plaque quantification by coronary computed tomography angiography using intravascular ultrasound as a reference standard: a comparison between standard and last generation computed tomography scanners. *Eur Heart J Cardiovasc Imaging.* 2020;21:191-201.

61. Lee SE, Chang HJ, Sung JM, Park HB, Heo R, Rizvi A, Lin FY, Kumar A, Hadamitzky M, Kim YJ, Conte E, Andreini D, Pontone G, Budoff MJ, Gottlieb I, Lee BK, Chun EJ, Cademartiri F, Maffei E, Marques H, Leipsic JA, Shin S, Choi JH, Chinnaiyan K, Raff G, Virmani R, Samady H, Stone PH, Berman DS, Narula J, Shaw LJ, Bax JJ, Min JK. Effects of Statins on Coronary Atherosclerotic Plaques: The PARADIGM Study. *JACC Cardiovasc Imaging.* 2018;11:1475-84.

62. van Rosendael AR, van den Hoogen IJ, Gianni U, Ma X, Tantawy SW, Bax AM, Lu Y, Andreini D, Al-Mallah MH, Budoff MJ, Cademartiri F, Chinnaiyan K, Choi JH, Conte E, Marques H, de Araújo Gonçalves P, Gottlieb I, Hadamitzky M, Leipsic JA, Maffei E, Pontone G, Shin S, Kim YJ, Lee BK, Chun EJ, Sung JM, Lee SE, Virmani R, Samady H, Sato Y, Stone PH, Berman DS, Narula J, Blankstein R, Min JK, Lin FY, Shaw LJ, Bax JJ, Chang HJ. Association of Statin Treatment With Progression of Coronary Atherosclerotic Plaque Composition. *JAMA Cardiol.* 2021;6:1257-66.

63. Shin S, Park HB, Chang HJ, Arsanjani R, Min JK, Kim YJ, Lee BK, Choi JH, Hong GR, Chung N. Impact of Intensive LDL Cholesterol Lowering on Coronary Artery Atherosclerosis Progression: A Serial CT Angiography Study. *JACC Cardiovasc Imaging.* 2017;10:437-46.

64. Puchner SB, Liu T, Mayrhofer T, Truong QA, Lee H, Fleg JL, Nagurney JT, Udelson JE, Hoffmann U, Ferencik M. High-risk plaque detected on coronary CT angiography predicts acute coronary syndromes independent of significant stenosis in acute chest pain: results from the ROMICAT-II trial. *J Am Coll Cardiol.* 2014;64:684-92.

65. Williams MC, Kwiecinski J, Doris M, McElhinney P, D'Souza MS, Cadet S, Adamson PD, Moss AJ, Alam S, Hunter A, Shah ASV, Mills NL, Pawade T, Wang C, Weir McCall J, Bonnici-Mallia M, Murrills C, Roditi G, van Beek EJR, Shaw LJ, Nicol ED, Berman DS, Slomka PJ, Newby DE, Dweck MR, Dey D. Low-Attenuation

Noncalcified Plaque on Coronary Computed Tomography Angiography Predicts Myocardial Infarction: Results From the Multicenter SCOT-HEART Trial (Scottish Computed Tomography of the HEART). *Circulation.* 2020;141:1452-62.

66. Andreini D, Conte E, Serruys PW. Coronary plaque features on CTA can identify patients at increased risk of cardiovascular events. *Curr Opin Cardiol.* 2021;36:784-92.

67. Budoff MJ, Bhatt DL, Kinninger A, Lakshmanan S, Muhlestein JB, Le VT, May HT, Shaikh K, Shekar C, Roy SK, Tayek J, Nelson JR. Effect of icosapent ethyl on progression of coronary atherosclerosis in patients with elevated triglycerides on statin therapy: final results of the EVAPORATE trial. *Eur Heart J.* 2020;41: 3925-32.

68. Nissen SE, Wolski K, Balog C, Swerdlow DI, Scrimgeour AC, Rambaran C, Wilson RJ, Boyce M, Ray KK, Cho L, Watts GF, Koren M, Turner T, Stroes ES, Melgaard C, Campion GV. Single Ascending Dose Study of a Short Interfering RNA Targeting Lipoprotein(a) Production in Individuals With Elevated Plasma Lipoprotein(a) Levels. *JAMA.* 2022;327:1679-87.

69. O'Donoghue ML, Fazio S, Giugliano RP, Stroes ESG, Kanevsky E, Gouni-Berthold I, Im K, Lira Pineda A, Wasserman SM, Češka R, Ezhov MV, Jukema JW, Jensen HK, Tokgözoğlu SL, Mach F, Huber K, Sever PS, Keech AC, Pedersen TR, Sabatine MS. Lipoprotein(a), PCSK9 Inhibition, and Cardiovascular Risk. *Circulation.* 2019;139:1483-92.

70. Bittner VA, Szarek M, Aylward PE, Bhatt DL, Diaz R, Edelberg JM, Fras Z, Goodman SG, Halvorsen S, Hanotin C, Harrington RA, Jukema JW, Loizeau V, Moriarty PM, Moryusef A, Pordy R, Roe MT, Sinnaeve P, Tsimikas S, Vogel R, White HD, Zahger D, Zeiher AM, Steg PG, Schwartz G S; ODYSSEY OUTCOMES Committees and Investigators. Effect of Alirocumab on Lipoprotein(a) and Cardiovascular Risk After Acute Coronary Syndrome. *J Am Coll Cardiol.* 2020;75:133-44.

71. Kaiser Y, Daghem M, Tzolos E, Meah MN, Doris MK, Moss AJ, Kwiecinski J, Kroon J, Nurmohamed NS, van der Harst P, Adamson PD, Williams MC, Dey D, Newby DE, Stroes ESG, Zheng KH, Dweck MR. Association of Lipoprotein(a) With Atherosclerotic Plaque Progression. *J Am Coll Cardiol.* 2022;79:223-33.

72. Lee JM, Choi G, Koo BK, Hwang D, Park J, Zhang J, Kim KJ, Tong Y, Kim HJ, Grady L, Doh JH, Nam CW, Shin ES, Cho YS, Choi SY, Chun EJ, Choi JH, Nørgaard BL, Christiansen EH, Niemen K, Otake H, Penicka M, de Bruyne B, Kubo T, Akasaka T, Narula J, Douglas PS, Taylor CA, Kim HS. Identification of High-Risk Plaques Destined to Cause Acute Coronary Syndrome Using Coronary Computed Tomographic Angiography and Computational Fluid Dynamics. *JACC Cardiovasc Imaging.* 2019;12:1032-43.

73. deSouza NM, Achten E, Alberich-Bayarri A, Bamberg F, Boellaard R, Clément O, Fournier L, Gallagher F, Golay X, Heussel CP, Jackson EF, Manniesing R, Mayerhofer ME, Neri E, O'Connor J, Oguz KK, Persson A, Smits M, van Beek EJR, Zech CJ; European Society of Radiology. Validated imaging biomarkers as decision-making tools in clinical trials and routine practice: current status and recommendations from the EIBALL* subcommittee of the European Society of Radiology (ESR). *Insights into Imaging.* 2019;10:87.

74. Kolossváry M, Karády J, Szilveszter B, Kitslaar P, Hoffmann U, Merkely B, Maurovich-Horvat P. Radiomic Features Are Superior to Conventional Quantitative Computed Tomographic Metrics to Identify Coronary Plaques With Napkin-Ring Sign. *Circ Cardiovasc Imaging.* 2017;10:e006843.

75. Lin A, Kolossváry M, Yuvaraj J, Cadet S, McElhinney PA, Jiang C, Nerlekar N, Nicholls SJ, Slomka PJ, Maurovich-Horvat P, Wong DTL, Dey D. Myocardial Infarction Associates With a Distinct Pericoronary Adipose Tissue Radiomic Phenotype: A Prospective Case-Control Study. *JACC Cardiovasc Imaging.* 2020;13: 2371-83.

76. Xu P, Xue Y, Schoepf UJ, Varga-Szemes A, Griffith J, Yacoub B, Zhou F, Zhou C, Yang Y, Xing W, Zhang L. Radiomics: The Next Frontier of Cardiac Computed Tomography. *Circ Cardiovasc Imaging.* 2021;14:e011747.

77. Collet C, Sonck J, Leipsic J, Monizzi G, Buytaert D, Kitslaar P, Andreini D, De Bruyne B. Implementing Coronary Computed Tomography Angiography in the Catheterization Laboratory. *JACC Cardiovascular Imaging.* 2021;14:1846-55.

78. Kočka V, Thériault-Lauzier P, Xiong TY, Ben-Shoshan J, Petr R, Laboš M, Buithieu J, Mousavi N, Pilgrim T, Praz F, Overtchouk P, Beaudry JP, Spaziano M, Pelletier JP, Martucci G, Dandona S, Rinfret S, Windecker S, Leipsic J, Piazza N. Optimal Fluoroscopic Projections of Coronary Ostia and Bifurcations Defined by Computed Tomographic Coronary Angiography. *JACC Cardiovasc Interv.* 2020;13: 2560-70.

79. Hong SJ, Kim BK, Cho I, Kim HY, Rha SW, Lee SH, Park SM, Kim YH, Chang HJ, Ahn CM, Kim JS, Ko YG, Choi D, Hong MK, Jang Y; CT-CTO Investigators. Effect of Coronary CTA on Chronic Total Occlusion Percutaneous Coronary Intervention: A Randomized Trial. *JACC Cardiovasc Imaging.* 2021;14:1993-2004.

80. Kikuta Y, Cook CM, Sharp ASP, Salinas P, Kawase Y, Shiono Y, Giavarini A, Nakayama M, De Rosa S, Sen S, Nijjer SS, Al-Lamee R, Petraco R, Malik IS,

Mikhail GW, Kaprielian RR, Wijntjens GWM, Mori S, Hagikura A, Mates M, Mizuno A, Hellig F, Lee K, Janssens L, Horie K, Mohdnazri S, Herrera R, Krackhardt F, Yamawaki M, Davies J, Takebayashi H, Keeble T, Haruta S, Ribichini F, Indolfi C, Mayet J, Francis DP, Piek JJ, Di Mario C, Escaned J, Matsuo H, Davies JE. Pre-Angioplasty Instantaneous Wave-Free Ratio Pullback Predicts Hemodynamic Outcome In Humans With Coronary Artery Disease: Primary Results of the International Multicenter iFR GRADIENT Registry. *JACC Cardiovasc Interv.* 2018;11: 757-67.

81. Patel MR, Jeremias A, Maehara A, Matsumura M, Zhang Z, Schneider J, Tang K, Talwar S, Marques K, Shammas NW, Gruberg L, Seto A, Samady H, Sharp ASP, Ali ZA, Mintz G, Davies J, Stone GW. 1-Year Outcomes of Blinded Physiological Assessment of Residual Ischemia After Successful PCI: DEFINE PCI Trial. *JACC Cardiovasc Interv.* 2022;15:52-61.

82. Kogame N, Takahashi K, Tomaniak M, Chichareon P, Modolo R, Chang CC, Komiyama H, Katagiri Y, Asano T, Stables R, Fath-Ordoubadi F, Walsh S, Sabaté M, Davies JE, Piek JJ, van Geuns RJ, Reiber JHC, Banning AP, Escaned J, Farooq V, Serruys PW, Onuma Y. Clinical Implication of Quantitative Flow Ratio After Percutaneous Coronary Intervention for 3-Vessel Disease. *JACC Cardiovasc Interv.* 2019;12:2064-75.

83. Sonck J, Nagumo S, Norgaard BL, Otake H, Ko B, Zhang J, Mizukami T, Maeng M, Andreini D, Takahashi Y, Jensen JM, Ihdayhid A, Heggermont W, Barbato E, Mileva N, Munhoz D, Bartunek J, Updegrove A, Collinsworth A, Penicka M, Van Hoe L, Leipsic J, Koo BK, De Bruyne B, Collet C. Clinical Validation of a Virtual Planner for Coronary Interventions Based on Coronary CT Angiography. *JACC Cardiovasc Imaging.* 2022;15:1242-55.

84. Kawashima H, Onuma Y, Andreini D, Mushtaq S, Morel MA, Masuda S, Taylor CA, Bartorelli AL, Serruys PW, Pompilio G. Successful Coronary Artery Bypass Grafting Based Solely on Non-Invasive Coronary Computed Tomography Angiography. *Cardiovasc Revasc Med.* 2021;40S:187-9.

85. Sadeghi AH, Bakhuis W, Van Schaagen F, Oei FBS, Bekkers JA, Maat APWM, Mahtab EAF, Bogers AJJC and Taverne YJHJ. Immersive 3D virtual reality imaging in planning minimally invasive and complex adult cardiac surgery. *Eur Heart J - Digital Health.* 2020;1:62-70.

86. Schaap M, van Walsum T, Neefjes L, Metz C, Capuano E, de Bruijne M, Niessen W. Robust shape regression for supervised vessel segmentation and its application to coronary segmentation in CTA. *IEEE Trans Med Imaging.* 2011;30:1974-86.

87. Abbara S, Blanke P, Maroules CD, Cheezum M, Choi AD, Han BK, Marwan M, Naoum C, Norgaard BL, Rubinshtein R, Schoenhagen P, Villines T, Leipsic J. SCCT guidelines for the performance and acquisition of coronary computed tomographic angiography: A report of the society of Cardiovascular Computed Tomography Guidelines Committee: Endorsed by the North American Society for Cardiovascular Imaging (NASCI). *J Cardiovasc Comput Tomogr.* 2016;10:435-49.

88. Taylor CA, Fonte TA, Min JK. Computational fluid dynamics applied to cardiac computed tomography for noninvasive quantification of fractional flow reserve: scientific basis. *J Am Coll Cardiol.* 2013;61:2233-41.

89. Williams MC, Earls JP, Hecht H. Quantitative assessment of atherosclerotic plaque, recent progress and current limitations. *J Cardiovasc Comput Tomogr.* 2022;16:124-37.

90. Khav N, Ihdayhid AR, Ko B. CT-Derived Fractional Flow Reserve (CT-FFR) in the Evaluation of Coronary Artery Disease. *Heart Lung Circ.* 2020;29:1621-32.

Supplementary data

Supplementary Table 1. Anatomical diagnostic performance of CCTA with ICA as a standard reference.

Supplementary Table 2. Functional diagnostic performance of CCTA and CT-derived FFR with invasive FFR as a standard reference.

Supplementary Figure 1. Trials map.

Supplementary Figure 2. CCTA findings and clinical outcomes stratified by pretest probability.

Supplementary Figure 3. Fagan nomogram applying likelihood ratios to a pretest probability to calculate the post-test probability.

Supplementary Figure 4. Physiological indexes and interrogated coronary domain.

Supplementary Figure 5. Traditional chest pain diagnostic work-flow and the "one-stop shop" CCTA approach.

Supplementary Figure 6. Coronary plaque inflammation, IVUS-like imaging on CCTA and comparison with IVUS.

Supplementary Figure 7. PCI-Planner projection provided by CCTA.

Moving image 1. Preoperative holographic visualisation derived from CCTA as a preoperative planning tool and intraoperative support.

Moving image 2. Postoperative 3D digital model derived from CCTA.

The supplementary data are published online at:
https://eurointervention.pcronline.com/
doi/10.4244/EIJ-D-22-00776

Supplementary data

Supplementary Table 1. Anatomical diagnostic performance of CCTA with ICA as a standard reference.

| Study/Author	Reference standard (ICA)	Year	Number of Patients	Sensitivity	Specificity	PPV	NPV	+LR	-LR	Accuracy
ACCURACY (Budoff MJ et al.)	≥50%	2008	230	95	83	64	99	5.56	0.06	NA
Meijboom WB et al.	≥50%	2008	360	99	64	86	97	2.76	0.01	88
MINISCAD (Marano R et al.)	>50%	2009	327	94	88	91	91	7.83	0.07	91
CORE-64 (Arbab-Zadeh A et al.)	≥50%	2012	273	91	87	9	88	7.00	0.10	NA
EVINCI (Neglia D et al.)	>70%, 30-70% with FFR ≤0.80, or LM >50%	2015	475	91	92	83	96	11.38	0.10	91
Budoff MJ et al.	>50%	2017	77	85	90	81	92	8.50	0.17	NA
PICTURE (Budoff MJ et al.)	≥50%	2017	230	92	78	82	90	4.18	0.10	NA
Andreini D et al.: Patients with atrial fibrillation	>50%	2017	83	95	98	95	98	39.00	0.05	96
Andreini D et al.: Patients with heart rate ≥80bpm	>50%	2018	40	100	82	100	82	5.56	0	90
Motoyama S et al.: UHR-CT, Median CACS 171	≥75%	2018	59	100	80	94	100	5.00	0	NA
Takagi H et al.: UHR-CT, Median CACS 250	≥50%	2018	38 Vessels: 113	100 96	67 81	94 80	100 96	3.00 4.96	0 0.05	95 88
VERDICT: NSTEACS (Linde JJ et al.)	≥50%	2020	1,023	97	72	91	88	3.49	0.05	89
Latina J et al. [15]: UHR-CT, Median CACS 1205	≥70%	2021	15 Vessels: 86	100 86	100 88	100 70	100 95	- 7.17	0 0.16	NA NA
CREDENCE: AI-QCT (Griffin WF et al.[19])	≥50% ≥70%	2022	303	94 94	68 82	81 69	90 97	2.94 5.22	0.09 0.07	84 86

AI-QCT: artificial intelligence-enabled quantitative coronary computed tomography angiography; CACS: coronary artery calcium score; CCTA: coronary computed tomographic angiography; ICA: invasive coronary angiography; NPV: negative predictive value; NSTEACS: non-ST-segment-elevation acute coronary syndrome; PPV: positive predictive value; UHR-CT: ultra-high-resolution CT; -LR: negative likelihood ratio; +LR: positive likelihood ratio.

Supplementary Table 2. Functional diagnostic performance of CCTA and CT-derived FFR with invasive FFR as a standard reference.

Study	Year	Design	Vessels	Accuracy (%)		Sensitivity (%)		Specificity (%)		PPV (%)		NPV (%)		AUC	
				CCTA	CT-FFR	CCTA	CT-FFR	CCTA	CT-FFR	CCTA	CT-FFR	CCTA	CT-FFR	CCTA	CT-FFR
HeatFlow FFR$_{CT}$															
DISCOVER-FLOW (Koo B-K et al.)	2011		159	59	84	91	88	40	82	47	74	89	92	0.73	0.90
DeFACTO (Min JK,et al.)	2012	Prospective Multi-centre	407	NA	NA	NA	80	NA	61	NA	NA	NA	NA	NA	NA
NXT (Nørgaard BL et al.)	2014		484	65	86	83	84	60	86	33	61	92	95	0.79	0.93
PACIFIC (Driessen RS et al. [27])	2019	Prospective Single centre	505	79	87	68	90	83	86	57	65	86	96	0.83	0.94
Siemens cFFR															
Renker M et al.	2014		67	NA	NA	90	85	34	85	37	71	89	93	0.72	0.92
Coenen A et al.	2016	Retrospective Single centre	189	56	75	81	88	38	65	49	65	73	88	0.64	0.83
De Geer J et al.	2016		23	NA	78	NA	83	NA	76	NA	56	NA	93	NA	NA
Kruk M et al.	2016	Prospective Single centre	96	44	74	100	76	2	72	43	67	100	80	0.66	0.84
Yang DH et al.	2017		138	78	81	94	87	66	77	64	71	94	90	0.86	0.89
Coenen A et al. Machine Learning-cFFR	2018	Retrospective Multi-centre	525	58	78	88	81	38	76	49	70	83	85	0.69	0.84
Canon CT-FFR															
Ko BS et al.	2017	Prospective Single centre	58	78	84	79	78	74	87	60	74	88	89	0.77	0.88
Ihdayhid AR et al.	2018	Prospective Single centre	84	73	88	86	81	66	84	56	71	90	90	0.76	0.89
Fujimoto S et al.	2019		104	55	84	71	91	43	78	48	76	67	92	057	0.85
Pulse CT-QFR															
Li Z et al.	2020	Retrospective Multi-centre	156	NA	87	NA	88	NA	87	NA	83	NA	91	NA	NA
Westra J et al.	2021		284	NA	80	NA	70	NA	87	NA	81	NA	79	NA	0.86

Supplementary Figure 1. Trials map.

CABG: coronary artery bypass graft; Coronary Computed Tomographic Angiography: CCTA; CTP: computed tomography perfusion; FFRCT: Fractional flow reserve derived from coronary computed tomographic angiography; PCI: percutaneous coronary intervention; PET: positron emission tomography; PTP: pre-test probability; SPECT: single-photon emission computed tomography. Abbreviations of trials; ADVANCE: Assessing Diagnostic Value of Non-invasive FFRCT in Coronary Care; AMPLIFiED: Assessment of Myocardial Perfusion Linked to Infarction and Fibrosis Explored With Dual-Source CT; CATCH-2: CArdiac cT in the treatment of acute Chest Pain 2; CONFIRM: Coronary CT Angiography

Evaluation for Clinical Outcomes: An International Multicenter; CORE320: 320-row Multi-detector Computed Tomography Angiography and Myocardial Perfusion; CRESCENT II: Comprehensive Cardiac CT Versus Exercise Testing in Suspected Coronary Artery Disease II; CRISP-CT: Cardiovascular RISk Prediction using Computed Tomography; DISCHARGE: Diagnostic Imaging Strategies for Patients with Stable Chest Pain and Intermediate Risk of Coronary Artery Disease; EMERALD: Exploring the Mechanism of Plaque Rupture in Acute Coronary Syndrome Using Coronary CT Angiography and Computational Fluid Dynamic; EVAPORATE: Effect of Vascepa on Improving Coronary Atherosclerosis in People With High Triglycerides Taking Statin Therapy; FORECAST: Fractional Flow Reserve-Derived From Computed Tomography Coronary Angiography in the Assessment and Management of Stable Chest Pain; FOURIER: Further Cardiovascular Outcomes Research with PCSK9 Inhibition in Subjects with Elevate Risk; NXT: Analysis of Coronary Blood Flow Using Coronary CT Angiography, Next steps; PACIFIC: Prospective Comparison of Cardiac PET/CT, SPECT/CT Perfusion Imaging and CT Coronary Angiography With Invasive Coronary Angiography; ODYSSEY Outcomes; Evaluation of Cardiovascular Outcomes After an Acute Coronary Syndrome During Treatment With Alirocumab; PARADIGM: Progression of AtheRosclerotic PlAque Determined by Computed TomoGraphic Angiography Imaging; PERFECTION: PERfusion Versus Fractional Flow Reserve CT Derived In Suspected CoroNary; PROMISE: Prospective Multicenter Imaging Study for Evaluation of Chest Pain; P3: Precise Percutaneous Coronary Intervention Plan; ROMICAT II: Rule Out Myocardial Infarction/Ischemia Using Computer Assisted Tomography II; SCAPIS: Swedish Cardiopulmonary Bioimage Study; SCOT-HEART: Scottish Computed Tomography of the Heart; SPECIFIC: Dynamic Stress Perfusion CT for Detection of Inducible Myocardial Ischemia; SYNTAX: Synergy Between Percutaneous Coronary Intervention With Taxus and Cardiac Surgery.
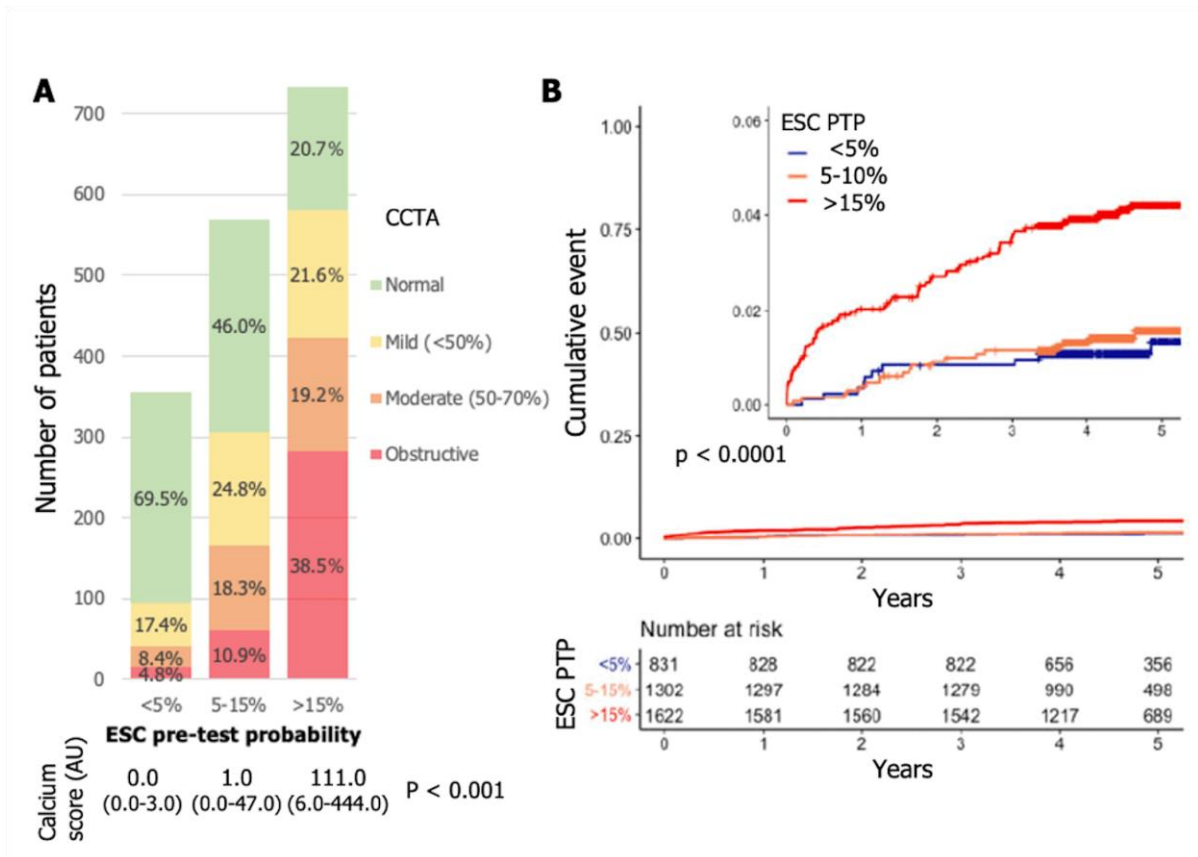
Supplementary Figure 2. CCTA findings and clinical outcomes stratified by pretest probability.

(A) CCTA findings and **(B)** cumulative incidence of cardiovascular death or non-fatal myocardial infarction over 5 years stratified by European Society of Cardiology (ESC) pre-test probability (PTP) categories in the SCOT HEART study. Reproduced with permission from Bing R et al. [7]. AU: Agatston units.
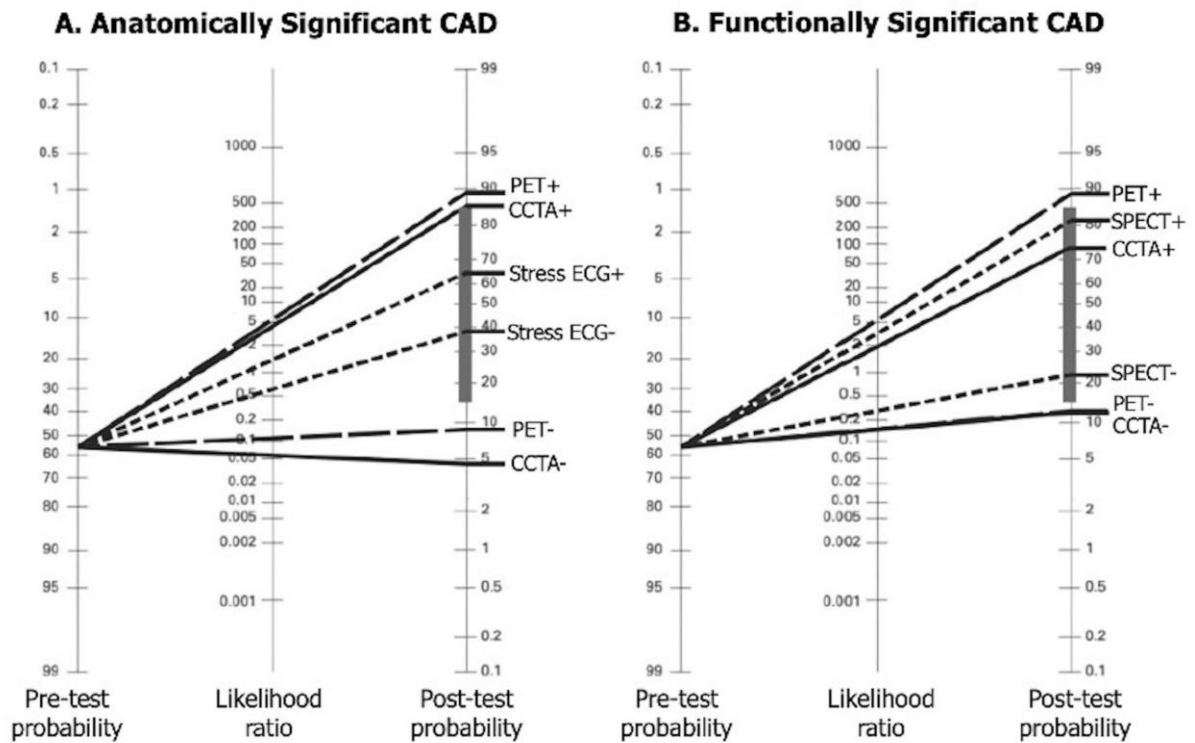
Supplementary Figure 3. Fagan nomogram applying likelihood ratios to a pretest probability to calculate

the post-test probability.

The gray bars show the range of post-test probability in which coronary artery disease cannot confidently ruled-in or ruled-out (post-test probability: 15-85%). **(A)** Stress echocardiogram (ECG) cannot rule-in or rule-out while CCTA and PET can. **(B)** SPECT cannot rule-in or rule-out. On the other hand, CCTA can only rule-out, and PET can both. Modified with permission from Knuuti J et al[14]. Abbreviation as in **Supplementary Figure 1**.
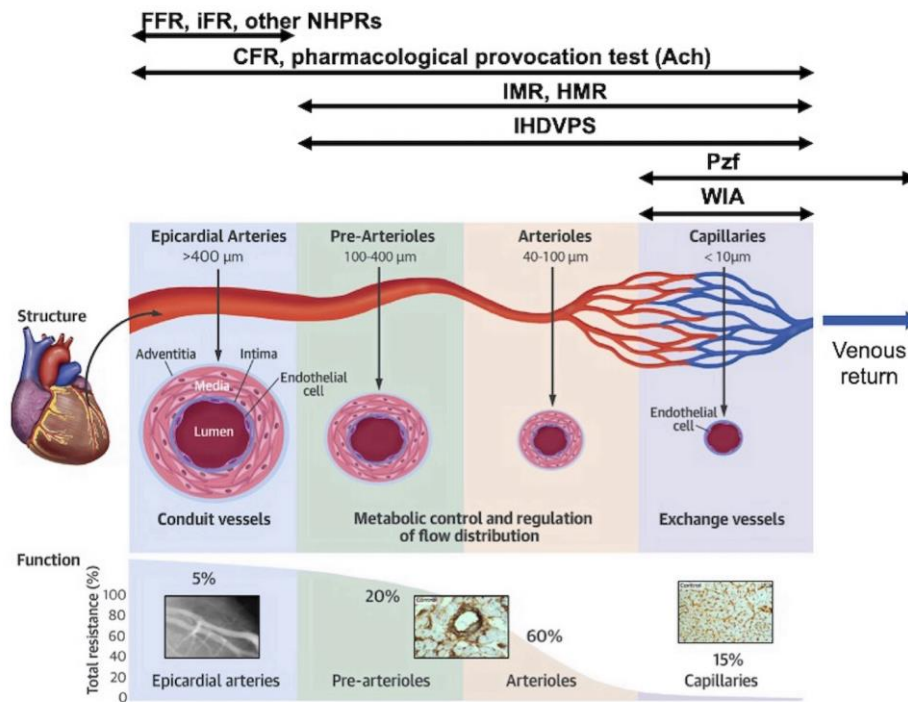
Supplementary Figure 4. Physiological indexes and interrogated coronary domain.

Normal structure and function of the coronary macro- and microcirculation and corresponding fields of physiological assessment techniques. Reproduced with permission from Kogame N et al. [47]. Ach: acetylcholine; CFR: coronary flow reserve; HMR: hyperemic microvascular resistance; iFR: instantaneous wave-free ratio; IHDVPS: instantaneous hyperemic diastolic velocity pressure slope; IMR: index of microvascular resistance; NHPR: no hyperemic pressure ratio; Pzf: zero flow pressure; WIA: wave-intensity analysis
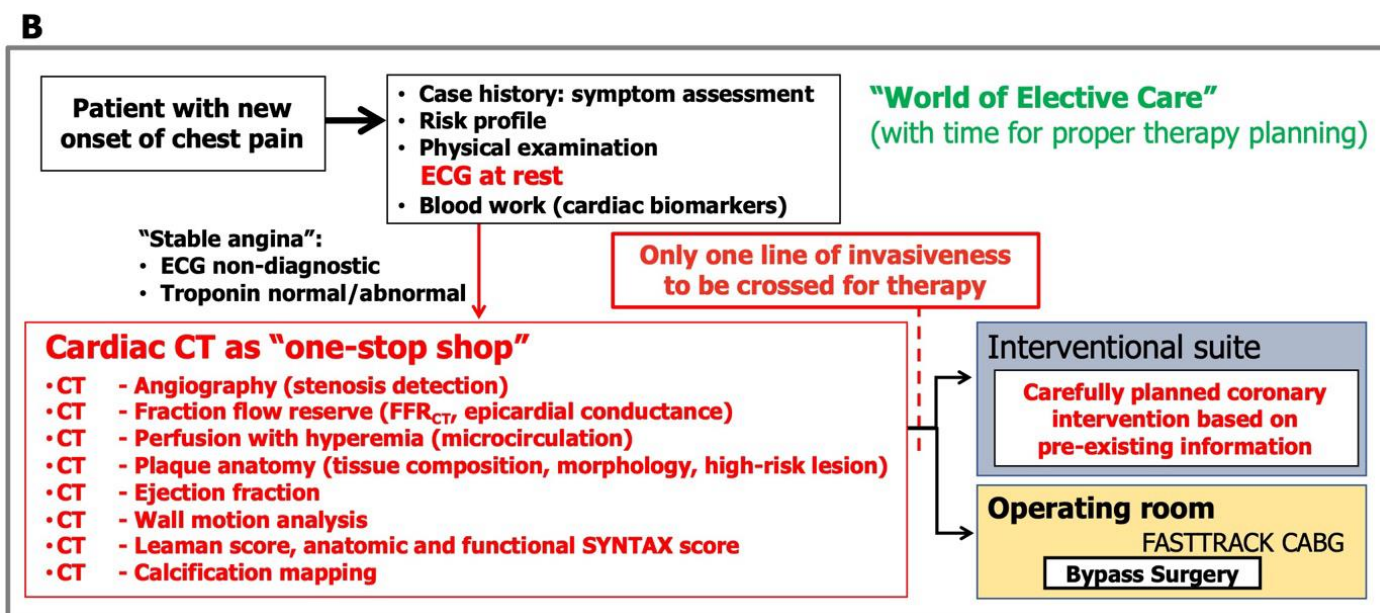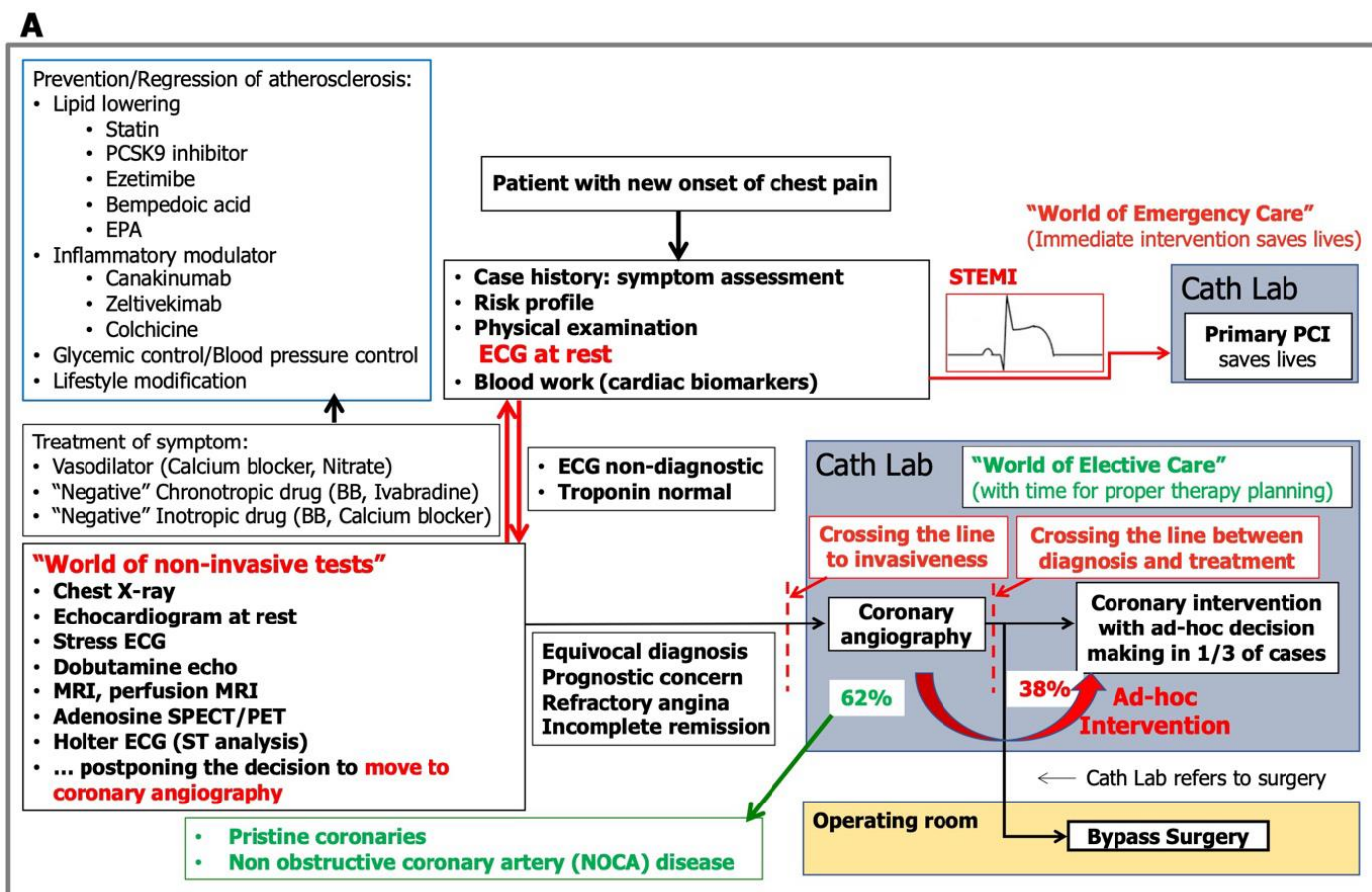
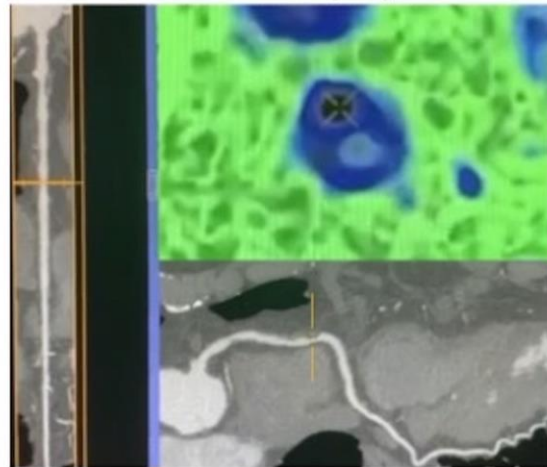**Supplementary Figure 5.** Traditional chest pain diagnostic workflow and the "one-stop shop" CCTA approach.

(A) In the NCDR CathPCI Registry, 38% of patients undergoing elective invasive coronary angiography (ICA) received ad hoc PCI, whereas in 62%, ICA was not followed by revascularization (Patel MR et al.).

(B) Screening, diagnosis, decision-making and treatment planning are relying solely on CCTA. BB: β-blocker; EPA: eicosapentaenoic acid; MRI: magnetic resonance imaging; PCSK9: proprotein convertase substilisin kexin type-9; SPECT: single-photon emission computed tomography.
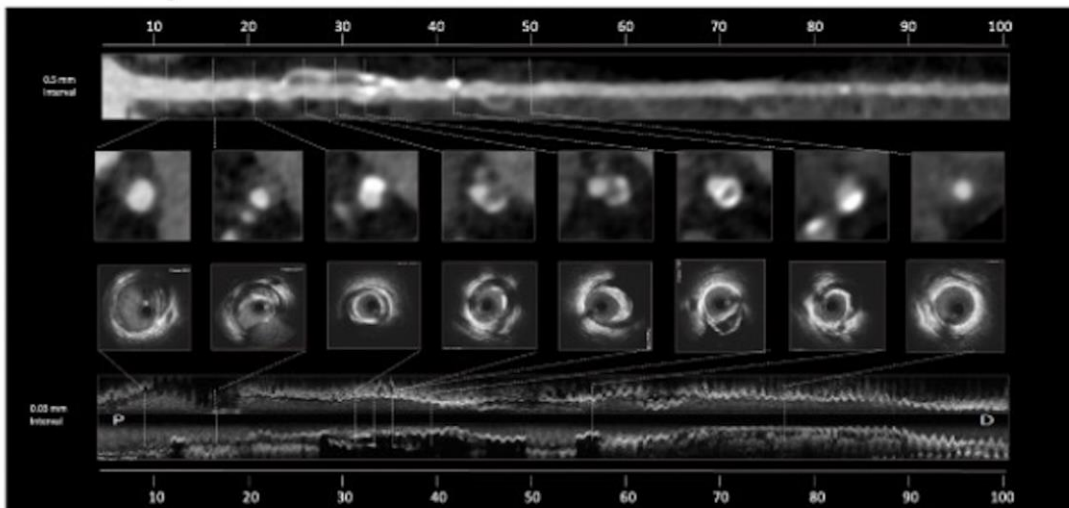
Supplementary Figure 6. Coronary plaque inflammation, IVUS-like imaging on CCTA and comparison

with IVUS.

(A) Coronary plaque inflammation detected by perivascular fat attenuation index (FAI). **(B)** IVUS-like

imaging of cross-section area of vessel atherosclerotic plaque provided by a virtual pullback on CCTA.

IVUS: intravascular ultrasonography; LAP: low attenuation plaque.
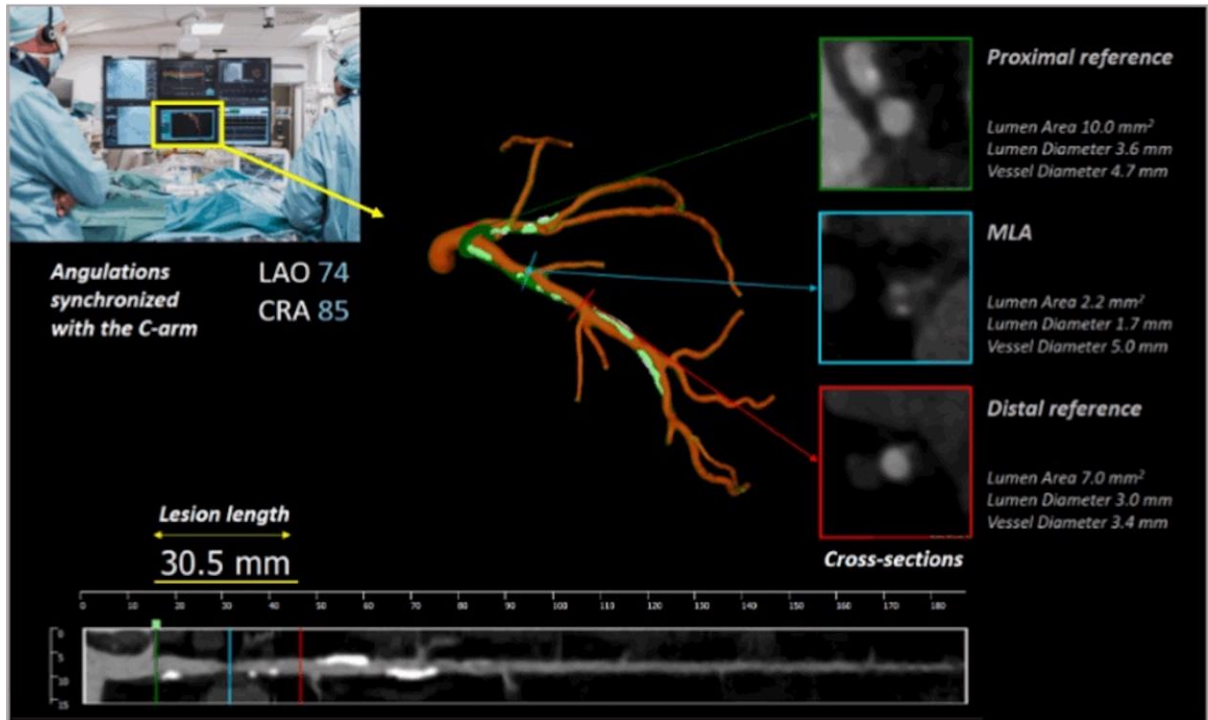
Supplementary Figure 7. PCI-Planner projection provided by CCTA.

Moving image 1, Moving image 2. Holographic visualisation and 3D modelling derived from CCTA as a preoperative planning tool and intraoperative support.

Preoperative holographic visualization **(Moving image 1)** and postoperative 3D digital model **(Moving image 2)** show how a surgeon can use CCTA images for planning and performing surgery. The 3D digital model **(Moving image 2)** demonstrates the possibility of using the right internal mammary artery (RIMA) as a graft implanted on the mid-part of the right coronary artery (RCA).